

MASTER THESIS PROJECT REPORT

Investment model for a Power-to-X plant over a 30-year period

SUPERVISORS

Rasmus Bo Bramstoft Pedersen, Assistant Professor, DTU Management
Nicolas Jean Bernard Campion, Postdoc Researcher, DTU Management
Marco Saretta, Industrial PhD, Rambøll, DTU

AUTHOR

Pablo Gutiérrez Mordini s222850

February 23, 2025

Acknowledgements

This project would have been nothing without all the people around me that pushed me forward and gave me the energy and motivation I needed to keep going.

Special thanks to Marco for all the help and support during all those 45-minute meetings that we had during the last six months. With you I not only learned the technical stuff but also about the importance of communication and be clear with what is wanted to express.

Thank you Nicolas, for being flexible an adapting the work to where I desired. I am aware that it might not were your comfort zone, but you always kept helping.

I also want to thank Rasmus, for being my main supervisor at DTU and allowed me to start the thesis under your department.

I do not want to forget Søren Møller Thomsen, who believed in me and gave me the opportunity to establish the collaboration with Rambøll.

To my mother who was always there, from the beginning to the very end (literally). Paula who always had something nice to say and fill me with energy. And Ñaño, for bearing together with stressful deadlines.

Finally, I want to thank Jonas, who was always happy to help and have infinite patience, Marco for his constant support and motivating messages, and Marina who was with me when I sent the email to Søren that set off the first domino.



Contents

1 Executive summary	1
2 Introduction	2
2.1 Motivation	2
2.2 Shipping fuel. Compatibility with current industry	2
2.3 Research question	3
2.4 Method overview	3
3 Methanol plant design	5
4 Demand market. Location identification. Resource assessments	9
4.1 Demand	9
4.2 Location identification	9
4.3 Wind and Solar resource	11
4.4 Electricity prices	11
4.5 CO_2 availability	12
4.6 Electrolyzer. Water availability	13
5 Costs review. Data inputs	14
5.1 Associated cost for each asset and technology specifics	14
5.2 Variable Renewable Energy	22
5.3 Electricity and CO_2 pricing	23
5.4 Financial parameters	24
6 Model formulation. Decomposition techniques	25
6.1 Mathematical model	26
6.2 Decomposition techniques	29
6.2.1 Benders	31
6.2.2 Dantzig-Wolfe	35
7 Results	38
7.1 Output production and operation of the plant	38
7.2 Comparison of the two model configurations	43
7.3 Levelized Cost of Methanol (LCOM)	47
7.4 Results related to decomposition techniques	48
7.5 Computational values	51
8 Sensitivity analysis	52
8.1 Grid connection	52
8.2 Electricity prices	53
9 Limitations and possible improvements	54
10 Conclusion	55



1 Executive summary

This study develops an optimization model to determine the optimal asset sizing for a methanol production plant over a 30-year period. The model aims to minimize total costs while ensuring the efficient and sustainable production of methanol. The research is motivated by the need for decarbonization in the shipping industry, where methanol presents a promising alternative fuel due to its compatibility with existing infrastructure and relatively lower emissions.

The optimization framework incorporates a detailed representation of asset investments, including renewable electricity generation, hydrogen production, CO₂ capture, and methanol synthesis. A significant portion of capital expenditure (56%–74%) is allocated to electricity production, with wind and solar capacities remaining stable across different model configurations. The study also explores two decomposition techniques: Benders and Dantzig - Wolfe decomposition. While Dantzig-Wolfe decomposition faced infeasibility issues due to state-of-charge (SOC) constraints for the storages, Benders decomposition proved computationally feasible but highly demanding. The latter technique may provide greater benefits in stochastic optimization scenarios, where the problem naturally decomposes into multiple subproblems.

Grid connection was identified as a crucial factor in cost minimization. A scenario with limited grid access led to significant oversizing of renewable generation assets, increasing capital expenditure. A sensitivity analysis suggested that maintaining a minimum grid connection of 30 MW would be optimal, while further expansion beyond this threshold would not result in substantial cost reductions. The Levelized Cost of Methanol (LCOM) was estimated at 1387 €/ton with grid connection and 2558 €/ton in the off-grid model configuration, aligning with external references.

The study also highlights the limited role of certain assets. Hydrogen storage tanks and Na-Cl batteries were found to be uneconomical due to their high costs. Auxiliary equipment, such as desalinating, heaters, and compressors, had a minimal impact on system performance and could be excluded from future implementations to simplify the model.

From an energy perspective, electricity curtailment was significantly higher in the off-grid configuration (66%) compared to the grid-connected case (12%), emphasizing the challenge of integrating variable renewable energy sources. The analysis of electricity price sensitivity showed that investment decisions were more influenced by grid electricity availability rather than price fluctuations. Even when electricity prices were doubled, total investment costs increased by only 4%, demonstrating that the model is robust to electricity price volatility.

Finally, the study provides a strong foundation for future research on stochastic optimization and improved energy market integration, ensuring the feasibility of large-scale methanol production under variable renewable energy conditions. By refining asset sizing strategies and optimizing grid interactions, future work can further enhance cost efficiency and operational flexibility. The results emphasize the importance of balancing renewable generation, storage, and grid connectivity to achieve a sustainable and economically viable Power-to-X system.



2 Introduction

2.1 Motivation

Addressing climate change and advancing decarbonization are essential for protecting our planet and ensuring sustainable growth. Climate change, fuelled by greenhouse gas emissions, threatens ecosystems, economies, and human health. Decarbonization - through cleaner energy, efficiency, and technologies such as Power-to-X (PtX) - is the key to mitigating these effects. Global achievements, like the Paris Agreement, which aims to limit global warming to 1.5°C, highlight international efforts to combat climate change[1]. However, for real progress, this transition must be economically feasible. Affordable, scalable solutions make it easier for industries and societies to adopt low-carbon practices without sacrificing economic stability. By balancing environmental goals with financial viability, we can create a prosperous and sustainable future for all.

Focusing on a relevant source of global Greenhouse Gases (GHG) emissions, international maritime transport accounts for 90% of global trade and almost 3% GHG emissions [2][3]. Emphasizing the economic importance and environmental impact of the sector highlights the urgent need for innovation and sustainable practices in maritime transport to balance global trade demands with climate goals. By 2050, the International Maritime Organization (IMO)[4] targets reducing the carbon intensity and GHG emissions of shipping by 70% and 50%, respectively, compared to 2008. Furthermore, large companies such as Maersk have set themselves the goal of becoming net-zero by 2040.[5][6]

2.2 Shipping fuel. Compatibility with current industry

The path towards decarbonization encompasses biofuels that may come from renewable energy sources. Because of that, PtX technologies are to become even more necessary towards decarbonization. Many different possibilities have been considered for this purpose. These were the main ones:: Ammonia, Methanol, Dimethyl ether, bio-LNG[7]. In order to make the selection, comparisons based on the Technology Readiness Levels (TRL) and the production costs were made. [8]

Due to its compatibility with existing engine technologies, Methanol was chosen as the fuel to be produced, which allows for a smoother transition to cleaner fuels without requiring significant modifications to ships[9]. Additionally, e-methanol is safer to handle than alternatives like ammonia or hydrogen, as it is less toxic and easier to store. Its global availability potential, combined with regulatory support for cleaner shipping fuels, makes e-methanol a practical and scalable solution for achieving sustainability in maritime transport. It is worth mentioning that Ammonia was the most ambitious option towards net zero, as it lacks carbon particles, but due to its Technology Readiness Level, it was discarded. [10][11]

In order to produce large amounts of methanol, it is necessary to have a comprehensive and detailed approach that addresses both the demand side and the optimal sizing and integration of production assets. Understanding the demand for methanol, particularly as a sustainable fuel in industries like shipping, is essential to determine the scale of production and infrastructure needed. Equally important is the design and sizing of assets, including wind and solar farms, electrolyzers, methanol reactors, and storage systems, to ensure efficient, cost-effective, and sustainable operations. Since the overarching goal is to decarbonize the sector, all energy used in methanol production should come from renewable sources such as wind and solar to minimize carbon footprints. Furthermore, as e-methanol contains carbon particles that are released into the atmosphere when burned, the integration of Carbon Capture Systems (CCS) is vital[12]. These systems ensure that the carbon required for methanol production is sourced — whether from industrial emissions or direct air capture — creating a circular carbon cycle that become carbon neutral or carbon negative. This approach enhances the environmental credibility of e-



methanol as a viable and scalable solution for reducing greenhouse gas emissions in shipping and other sectors. [13][14]

To achieve these objectives, it is essential to develop robust large-scale optimization models that enhance operational efficiency while minimizing costs. Methanol production involves complex interdependent processes, including hydrogen generation, carbon capture, and renewable energy integration, all of which require precise coordination to ensure feasibility and profitability. Given the complexity of these systems, decomposition techniques such as Benders decomposition and Dantzig-Wolfe decomposition provide powerful methods for solving large-scale optimization problems[15]. These techniques enable the breakdown of complex models into smaller, more manageable subproblems, improving computational efficiency and facilitating better decision-making. By applying these optimization approaches, it becomes possible to determine the optimal asset sizing and ensure economic feasibility.

2.3 Research question

Main question

How can large scale optimization models and decomposition techniques be applied to determine the optimal asset sizing for a Power-to-X plant over a 30-year horizon under variable renewable energy inputs?

Sub-question

How does grid connection availability influence asset dimensions and total investment cost in a Power-to-X methanol production system?

2.4 Method overview

The methodology used to determine the optimal sizing of assets in a methanol plant is grounded in minimizing the total cost of the power plant, implemented through a linear optimization model. This approach accounts for a wide range of costs that are integral to the development, operation, and sustainability of the plant. Initial investment costs, such as development expenditures (DEVEX) and capital expenditures (CAPEX), represent the upfront financial commitment required to establish the necessary infrastructure. Operational costs (OPEX), including maintenance, labor, and energy consumption, reflect the ongoing expenses associated with running the plant. In addition, abatement costs (ABEX) are considered to address the environmental impact, particularly in capturing and reducing carbon emissions, which are critical to achieving the decarbonization goals of the project. Furthermore, the cost of feedstocks, such as carbon dioxide (CO_2), has been incorporated, as the carbon used in methanol production need to be captured from sustainable sources to align with emissions reduction targets.

In large-scale optimization problems, such as those used to model a methanol plant, computational efficiency becomes a key challenge due to the high-dimensional nature of the problem. This is where decomposition techniques, like Benders and Dantzig-Wolfe decompositions, come into play [16]. These methods are invaluable in breaking down a complex problem into smaller, more tractable subproblems. By partitioning the optimization task, decomposition techniques enhance the scalability and robustness of the model, making it computationally feasible to tackle even the most intricate systems. This is especially critical in power plants that rely on variable renewable energy inputs, such as wind and solar power, where the supply can fluctuate due to weather conditions, and the energy market can be volatile. These uncertainties make it challenging to predict energy costs and consumption accurately over the plant's operational lifespan.

By applying decomposition, the optimization model can focus on solving smaller subproblems that represent specific aspects of the plant's operation or infrastructure, such as energy generation,



storage, or feedstock management. The solutions to these subproblems are then coordinated and integrated to provide a global optimal solution for the entire plant. This decomposition approach not only mitigates the computational burden of solving large-scale problems but also allows for more flexible and dynamic adaptation to changing conditions. For example, it facilitates adjustments to energy prices, fluctuations in renewable energy supply, or advancements in technology, ensuring the model remains responsive to evolving market and operational dynamics.

The application of decomposition techniques ensures that the optimization process is not only computationally efficient but also capable of generating solutions that are economically viable and environmentally sustainable. By enabling a dynamic response to uncertainties, these methods optimize long-term investment decisions and operational strategies for methanol production. This ensures that the plant operates efficiently, minimizes costs, and contributes to global decarbonization goals, making it a key component of sustainable and resilient energy systems in the future.

Benders decomposition is highly effective in handling scenarios with uncertainty by separating decision-making into two stages: a master problem that addresses strategic first-stage decisions, such as asset investments and sizing, and subproblems that capture second-stage scenarios, such as renewable energy variability and market price fluctuations. This two-stage approach is particularly advantageous for problems that naturally divide into long-term strategic and short-term operational decisions, as seen in methanol plant optimization. By focusing the master problem on long-term investments and leaving the subproblems to handle specific operational adjustments, Benders decomposition significantly reduces computational complexity while still accounting for uncertainties. Moreover, this method enables efficient scenario management, allowing for dynamic adaptation to changing conditions without overwhelming computational resources. When combined with scenario reduction techniques [17], Benders decomposition helps manage the "curse of dimensionality," ensuring that the methanol production system remains stable, adaptable, and optimized for both cost-efficiency and sustainability in uncertain environments.

Meanwhile, Dantzig-Wolfe decomposition is highly effective in handling large-scale, structured linear programs by reformulating the original problem into a master problem and smaller subproblems, allowing for more efficient solving through column generation. This approach is particularly useful in optimizing methanol production, where fluctuations in energy supply from renewable sources and volatile market prices introduce significant uncertainty. By managing each subproblem independently, Dantzig-Wolfe decomposition offers a structured way to handle the "curse of dimensionality" typically associated with stochastic optimization, ensuring that the system remains stable and convergent even under complex conditions. Stabilized versions of Dantzig-Wolfe decomposition, as outlined in research[18], further enhance the method's robustness and convergence, addressing instabilities in traditional stochastic methods. This makes the plant's operations more resilient, efficient, and computationally feasible, ensuring optimal performance even in fluctuating and uncertain scenarios.



3 Methanol plant design

Methanol is a final product synthesized from hydrogen (H_2) and carbon dioxide (CO_2). The primary objective of this report is to analyze the cost of methanol production under different electricity sourcing scenarios. The classification of methanol as blue or green depends on the source of electricity and CO_2 used in its production:

- Green methanol is a fully renewable methanol produced using hydrogen from electrolysis powered by renewable energy and CO_2 sourced from biogenic processes or Direct Air Capture (DAC). It qualifies as a Renewable Fuel of Non-Biological Origin (RFNBO) under EU regulations, meeting strict GHG reduction criteria. [19]
- Blue methanol is produced using hydrogen from renewable or fossil sources and CO_2 captured from fossil-based industrial emissions, such as CHP plants. While it reduces emissions compared to conventional methanol, it does not qualify as fully renewable under EU regulations. Instead, it is considered a transitional fuel, supporting decarbonization efforts by utilizing carbon capture.[19]

Since the grid energy mix typically includes fossil-fuel-based power generation, methanol produced using grid electricity cannot be fully classified as green, leading to its classification as blue methanol.

To begin with the production of the primary components required for methanol synthesis, hydrogen and carbon dioxide must be obtained. Among these, hydrogen production demands the most attention, as it can be highly expensive and offers multiple technological configurations. Since hydrogen is produced via an electrolyzer powered by electricity, the location of the renewable energy source in relation to the electrolyzer becomes a key factor in determining overall costs. Several configurations can be considered:

- Offshore Wind-Powered Electrolyzer: Placing an electrolyzer alongside an offshore wind farm would result in high infrastructure costs, as a specialized platform would be required. Additionally, transporting hydrogen via pipelines would add further expenses, making this option less economically viable.
- Solar-Powered Electrolyzer: If the electrolyzer is powered by solar panels, positioning them far from the consumption site would significantly increase investment costs, as extensive cabling infrastructure would be needed to transmit electricity over long distances.
- Decoupled Production and Consumption: Hydrogen does not necessarily need to be consumed on-site; it can be transported to its final destination. However, this also raises costs, as it would require expensive pipelines and dedicated hydrogen storage facilities at the end-use location.

Ultimately, the choice of hydrogen production strategy has a significant impact on overall costs. A careful evaluation of location, energy transmission, and transportation expenses is necessary to determine the most cost-effective and efficient configuration.

All the previously mentioned configurations, along with any additional feasible alternatives, should be analyzed in detail. To properly compare these options, feasibility studies would be conducted to assess their viability and ultimately determine the most optimal configuration. However, the focus of this report is not to conduct such an analysis, but rather to optimize the size of the assets within the power plant. As a result, certain assumptions will need to be made to simplify the modeling process. These assumptions are outlined in the following section.



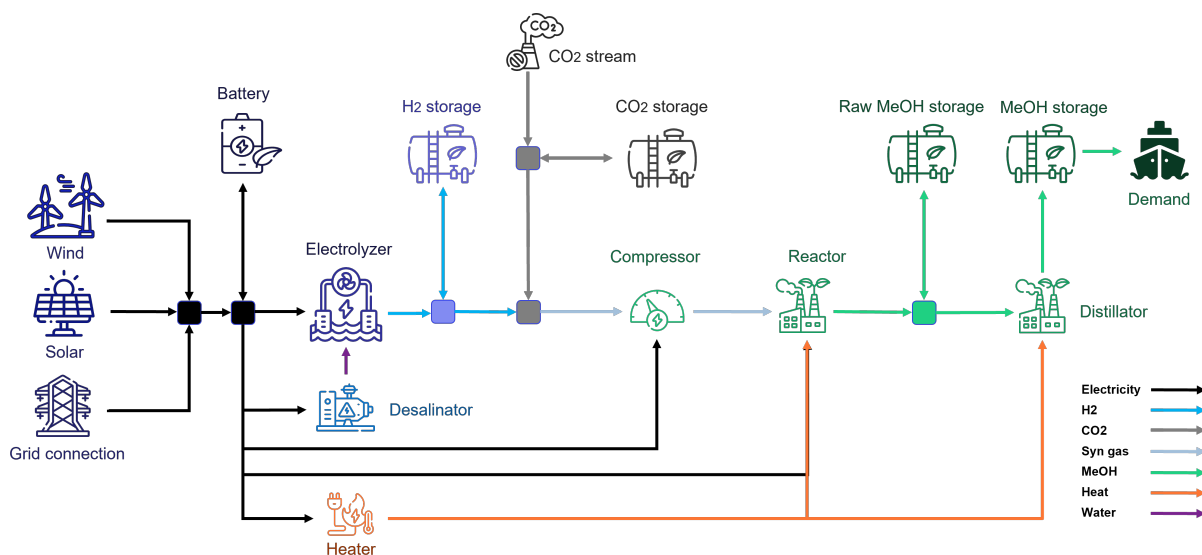


Figure 1: Methanol plant scheme

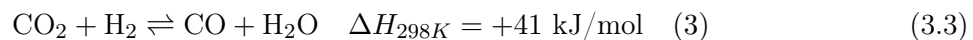
Although hydrogen is the most expensive component in methanol production, the source of carbon dioxide also requires careful consideration. It is essential to stay focused on the primary objective—producing renewable methanol. To achieve this, the CO_2 source must either be captured directly from the atmosphere or prevented from being emitted into the environment. This requirement stems from the fact that methanol, when used as a fuel, releases CO_2 . To prevent an overall increase in emissions, carbon must be captured and reintroduced into the production cycle, ensuring a net-zero carbon footprint. Two primary CO_2 sourcing methods are considered and will be analyzed in the next section:

1. Direct Air Capture (DAC) – Extracting CO_2 directly from the atmosphere.
2. Carbon Capture from a Combined Heat and Power (CHP) Plant – Capturing emissions from an industrial facility before they are released.

While the location and configuration of these carbon capture systems require further detailed study, assumptions and simplifications will be applied in this report to facilitate the optimization process.

Once the sources of hydrogen and carbon dioxide are established, the methanol production process can begin. Although the overall production pathway can be complex, certain simplifications have been made for the purpose of this report. At the core of the procedure, the synthesis gas (syngas) is first fed into the reactor, where raw methanol is produced. This raw methanol consists of a mixture of methanol and water. Since excess water content is undesirable, the next step involves a distillation column, where water is separated from methanol, leaving pure methanol as the final output.

Main equations for the process:



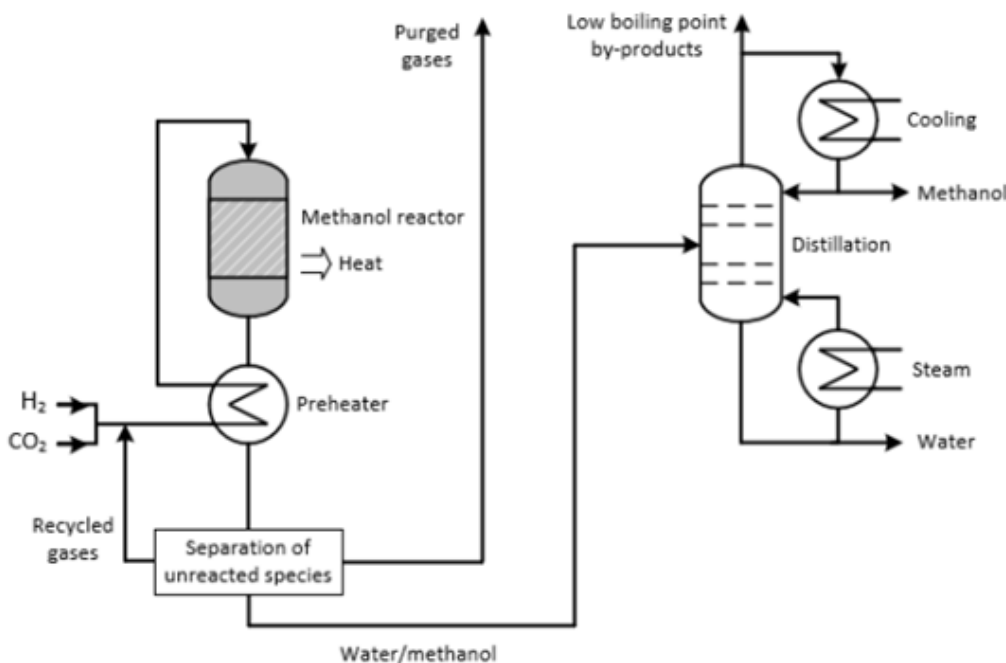


Figure 2: Simplified sketch of a hydrogen to methanol production plant.

Once the main process has been established, several auxiliary components become essential to ensure the smooth operation of the plant. These components primarily function as storage systems, which provide flexibility in plant operations. Without storage, the entire plant would need to operate at a constant output, which would - as it is shown below - raise significantly the costs. To enhance operational flexibility, five different storage systems have been considered. Each of them aims to improve different aspects of the plant's operation, but this does not imply that every storage system will necessarily be part of the final configuration. Since the objective of this report is to determine the optimal asset sizes, some storage capacities may be zero, meaning that certain storage systems might not be implemented. These storage systems play a crucial role in optimizing plant performance by managing fluctuations, enhancing flexibility, and reducing operational constraints. However, their inclusion in the final configuration depends on cost-effectiveness and overall system efficiency.

- **Battery Storage:** batteries provide flexibility in electricity usage, enabling the plant to store excess electricity generated by variable renewable energy sources and use it during periods of low availability.
- **Hydrogen Storage:** while electrolyzers offer considerable operational flexibility, they are more adaptable than the reactor. This means that the electrolyzer can adjust its operating point according to the availability of electricity, producing and storing excess hydrogen when the electricity supply is high. However, it is important to note that hydrogen storage systems are generally expensive.
- **CO₂ Storage Tank:** before carbon dioxide is mixed to produce syngas, it can be stored to help balance fluctuations in the reactor's operational levels.
- **Raw Methanol Storage:** the reactor has greater flexibility in adjusting its operational point than the distillation column. To improve plant optimization, an intermediate storage system for raw methanol can help manage fluctuations between these two processes.
- **Pure Methanol Storage:** before meeting methanol demand, the final product can be stored. As production can sometimes exceed demand, excess methanol can be stored to balance output and consumption over time.

The main components of the plant have been described already, but some additional assets are necessary for the correct working of the plant. These components are the: compressor, desalinator and heater.

- **Compressor:** prior to enter in the reactor, syn gas needs to be compressed in order to meet some specific conditions in terms of temperature and pressure. This has an impact on the model in a matter that making this compression requires additional demand of electricity.
- **Desalinator:** the electrolyzer requires water to work, as it would separate the molecules and then extract the hydrogen by an electrolysis process. This water needs to be treated previously, and therefore there will be an electricity demand associated with its consumption.
- **Heater:** both the reactor and the distillation column have a heating demand associated with their consumption. As a result, an auxiliary asset is set in turn would also require additional electricity demand



4 Demand market. Location identification. Resource assessments

Once the core structure of the investment model has been established, the next step is to provide the necessary input data. The primary objective of the model is to minimize the cost of producing a predetermined amount of methanol. If this production level were not specified, the model would naturally set all asset sizes to zero, being this result the lowest possible cost. To prevent this, a constant demand is enforced, ensuring that methanol production remains active. Following this, the location of the plant must be determined. In a comprehensive study, site selection would require an extensive evaluation, considering multiple potential locations alongside Environmental Impact Assessments. However, as mentioned above, site selection is not the focus of this study. Instead, both the plant location and renewable energy asset placement have been chosen based on simplified criteria. The chosen location, as detailed in the following sections, meets all necessary requirements while also offering access to valuable datasets that contribute to the robustness of the final results.

4.1 Demand

In the current landscape, Power-to-X technologies and the green transition are facing significant uncertainties, driven not only by economic factors but also by political influences that will shape the path toward decarbonization. As a result, many projects have been put on hold or even canceled altogether. A notable example is the cancellation of the FlagshipONE project in August 2024, which was developed by Ørsted and Liquid Wind AB[20][21]. This project represented a major investment in green e-methanol production, demonstrating its ambitious scale and importance in the sector. To replicate key characteristics of this project and establish baseline values, the demand used in this study has been set accordingly. Specifically, the annual methanol production target has been set at 50,000 tonnes, with production being evenly distributed across all operational hours of the plant.

Project details

The FlagshipONE project aimed to produce approximately 50,000 tonnes of e-methanol per year, relying on renewable hydrogen and biogenic CO_2 . The facility was designed to have an electrolyzer capacity of around 70 MW, enabling large-scale green methanol production. By the time of its cancellation, interest in e-methanol as a sustainable fuel had been growing significantly, with over 110 e-methanol vessels ordered or in operation, up from 80 at the end of 2022. [22]

The project was planned to be located on the grounds of the biomass-fired combined heat and power (CHP) plant Hörneborgsverket in Örnsköldsvik, Sweden. The e-methanol production would have been powered by renewable electricity, while biogenic carbon dioxide would have been captured from the Hörneborgsverket CHP plant. As a substitute for fossil fuels, the project had the potential to reduce CO_2 emissions in shipping by 100,000 tonnes per year. Additionally, Liquid Wind estimated that the facility would upcycle up to 70,000 tonnes of CO_2 annually.

Finally, hydrogen for the process would have been produced through electrolysis, powered by a 75 MW onshore wind facility. The overall plant was expected to generate 140 tonnes of renewable methanol per day, contributing significantly to decarbonization efforts in the maritime sector.

4.2 Location identification

The location of both the methanol plant and the renewable energy assets must meet certain requirements to ensure that cost estimations remain realistic and not overestimated. The plant will be powered by an offshore wind farm and the produced e-methanol will be used as fuel for shipping, a coastal location is necessary. This ensures proximity to both the energy source and shipping infrastructure, optimizing logistics and reducing additional transportation costs. Additionally, because offshore wind energy represents a significant portion of the total costs,



the selected location must meet two key criteria: it must be permitted for offshore wind farm development. and it must have high wind resources to ensure optimal power generation. The following two figures illustrate a map displaying the relative costs of offshore energy in different regions, and a list of potential locations for offshore wind farms.

Considering these factors, the chosen location for the methanol plant is near Esbjerg, as it meets the technical, logistical, and economic requirements for an optimal implementation.

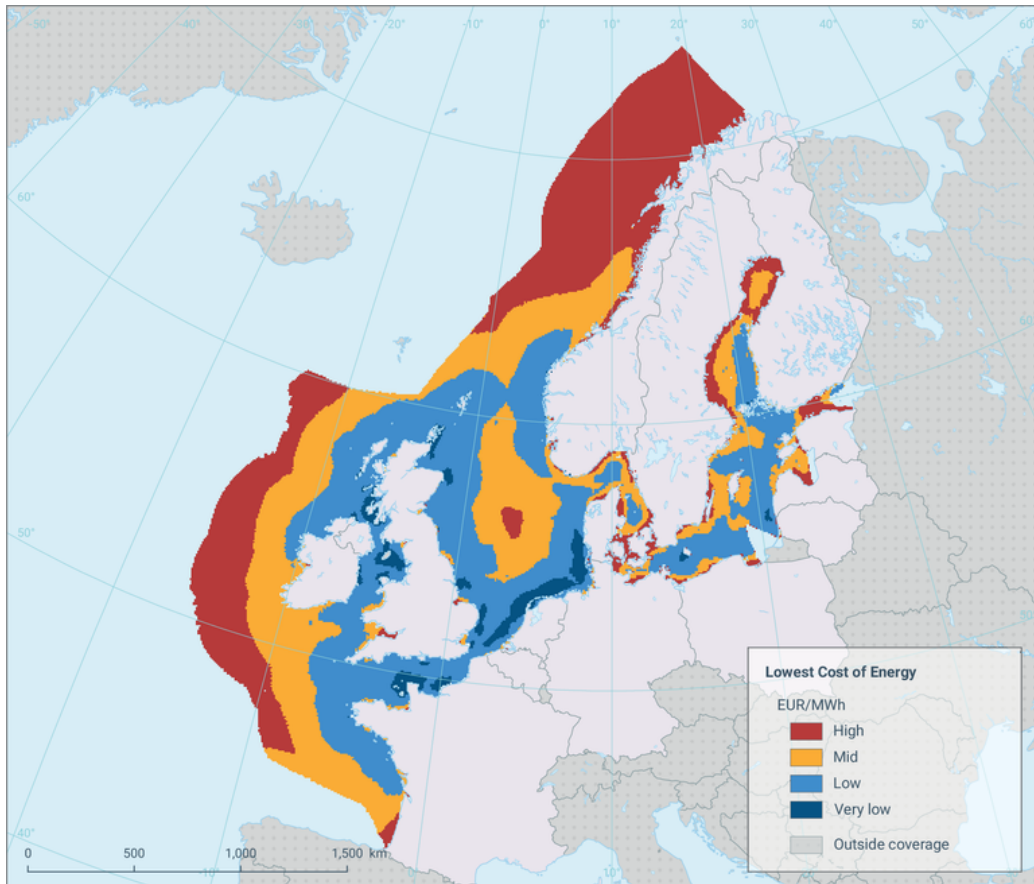


Figure 3: Relative lowest cost of offshore

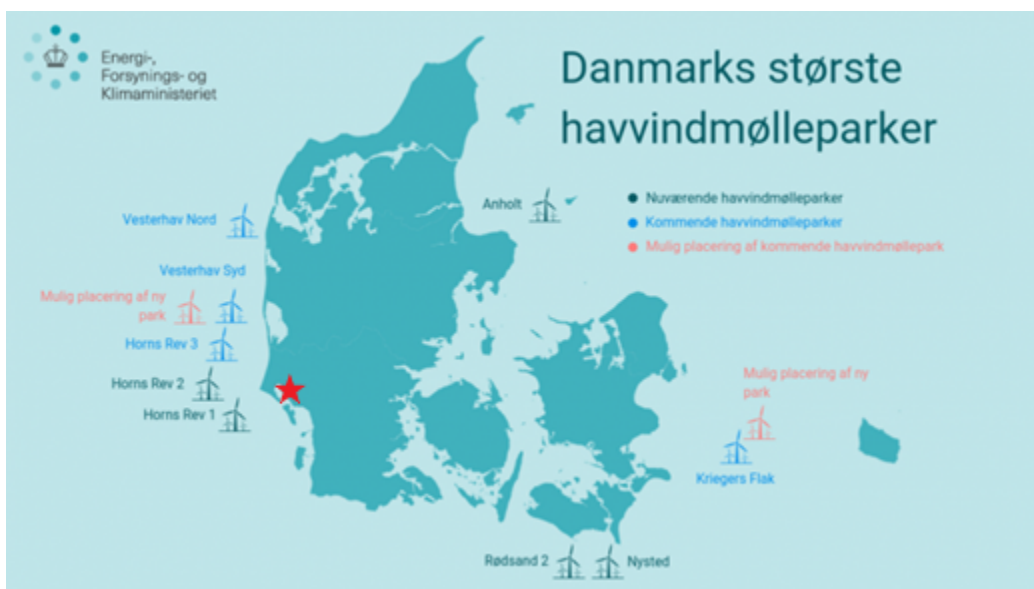


Figure 4: Possible locations for new offshore wind farm where Esbjerg is marked with a star

4.3 Wind and Solar resource

Once the **location** was selected, the next step involved retrieving historical data for the region. In this regard, an important assumption was made:

Wind and solar resources have remained unchanged over time, meaning that wind speeds and solar irradiance from the past 30 years are assumed to be representative of future conditions.

To obtain this historical data, Renewables Ninja was used as the primary source. However, when extracting data from Renewables Ninja, both wind and solar datasets require tuning to ensure realistic results. For instance, when retrieving wind data, the following parameters must be specified:

- Wind farm capacity
- Hub height
- Turbine model

These parameters were selected to match the capacity factor reported by The Danish Energy Agency, ensuring that the cost assumptions of these assets align with their actual levelized cost of energy (LCOE). This assumption and methodology were applied consistently to both wind and solar capacities, ensuring that the model remains cost-reflective and aligned with real-world energy production conditions.

4.4 Electricity prices

Unlike the assumption made for wind and solar resources, the same approach cannot be applied to electricity prices, as they tend to fluctuate over time and follow a general upward trend. Moreover, electricity prices are often influenced by renewable energy generation, particularly wind and solar production. The cross-correlation between wind, solar, and electricity prices over the past ten years provides insight into these relationships:

- A negative correlation exists between wind generation and both solar generation and electricity prices. This aligns with expectations, as higher wind generation generally leads to lower electricity prices and reduced solar output, and vice versa.
- However, solar generation shows no significant correlation with electricity prices. That can be attributed to the relatively low penetration of solar capacity in Denmark, meaning that its influence on electricity prices remains limited.

These trends emphasize the interaction between renewable energy availability and market electricity prices, highlighting the importance of accurate price modeling when determining asset sizing and operational strategies.



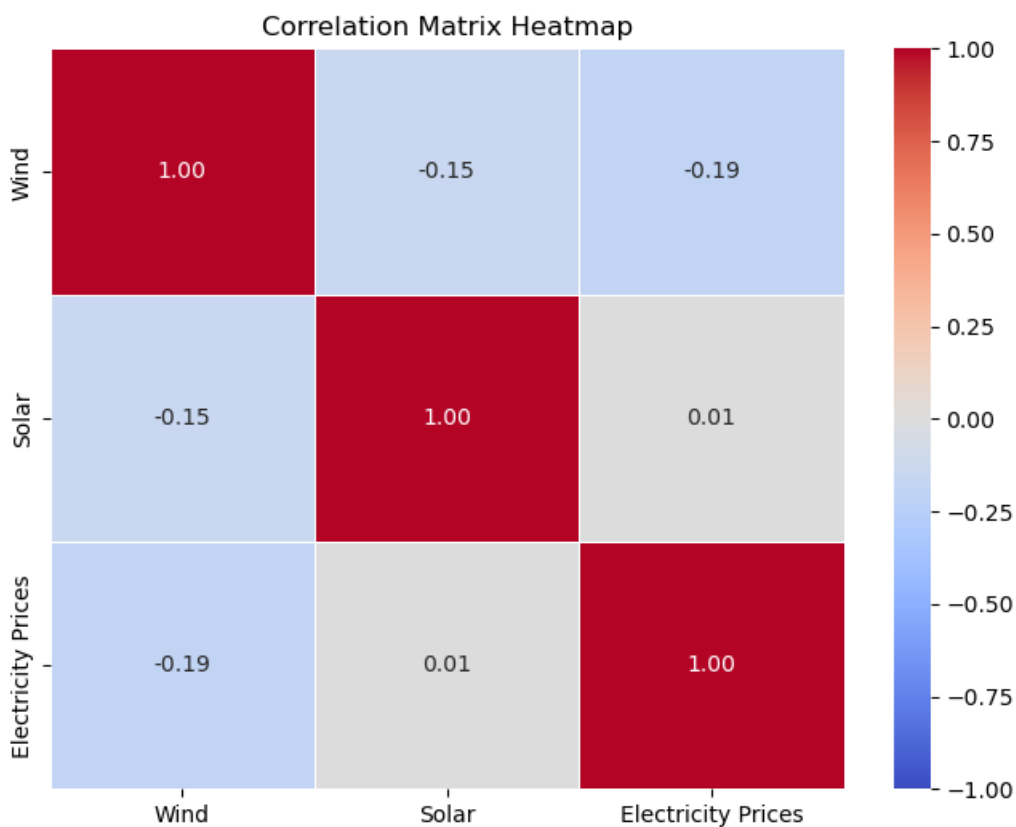


Figure 5: Correlation matrix heatmap

Accurately modeling electricity prices would require a detailed study, potentially using seasonal ARMA models that incorporate correlations with other relevant parameters. However, since the objective of this report is not to delve into advanced modeling projections of electricity prices, a simplification has been applied. Additionally, establishing a correlation between electricity prices and wind or solar production would introduce significant complexity, making it difficult to implement within the scope of this study. As a result, this correlation has not been included in the model. Instead, a simplified approach has been adopted:

- A random time series has been generated to represent electricity prices.
- The average value of this series is set equal to the mean electricity price from the past two years.
- Random noise has been added to reflect the natural fluctuations in electricity prices.

This approach should provide a reasonable approximation of electricity price behavior while keeping the model computationally manageable.

4.5 CO₂ availability

When planning the carbon dioxide source, it is essential to ensure a reliable and continuous supply. To achieve this, two main possibilities have been considered:

- **CO₂ from a Power Plant:** this approach provides a constant stream of CO₂ at a fixed price, feeding the methanol plant. The sustainability of this solution depends on the type of power plant. If CO₂ is sourced from biogas plants or waste-to-energy facilities, the process could be carbon-neutral or even carbon-negative. However, this solution is dependent on biomass or waste availability, which may impose supply limitations.

- **Direct Air Capture (DAC):** This method extracts CO_2 directly from ambient air through chemical absorption. While it presents a fully decarbonized solution, the main drawback is its high energy intensity, making it currently impractical in terms of energy costs and efficiency.

Given these considerations, a constant CO_2 supply from a CHP plant has been adopted as the preferred solution. While this approach may not always be carbon-neutral if fossil fuels are involved, it ensures:

- A stable and continuous CO_2 stream, which is critical for methanol production.
- The use of established carbon capture technology, reducing uncertainty.
- Alignment with the FlagshipONE project, which follows the same approach.

This choice balances feasibility, reliability, and technology maturity, ensuring that the methanol production process remains consistent and economically viable.

4.6 Electrolyzer. Water availability

In the study “*Water Electrolyzer Operation Scheduling for Green Hydrogen Production*”[23], four different electrolyzer technologies were compared:

- Alkaline Water Electrolysis (AWE)
- Proton Exchange Membrane Water Electrolysis (PEMWE)
- Solid Oxide Electrolysis Cell (SOEC)
- Anion Exchange Membrane Water Electrolysis (AEMWE)

The selection of the most suitable electrolyzer was based on several key factors, including: Technology readiness level (TRL), development stage, average efficiency, durability and Capital expenditure (CAPEX). Among all the technologies analyzed, AWE demonstrated the best overall performance, excelling in efficiency, durability, and cost-effectiveness. As a result, AWE was chosen as the preferred electrolyzer for this study. Below is a list of the key properties of the AWE electrolyzer, detailing its operational characteristics and performance metrics.

Type	Technology Readiness Level	Development Stage	Durability (Full Load Hours)	CAPEX (USD,\$)
AWE	TRL-9	More than 1 GW	60,000 – 100,000 h	500-1400/kW

Table 1: Specifications of the AWE Electrolyzer

In alignment with the chosen electrolyzer, a constant water supply is required to sustain hydrogen production. Given that the selected location for the methanol plant is near the sea, an abundant water source is available, ensuring that water extraction does not negatively impact the environment. However, the use of seawater presents a technical challenge: it must be processed before use to meet the purity requirements of the electrolyzer. To address this, a desalination unit must be integrated into the system, to ensure that the water supply is suitable for electrolysis and does not compromise equipment performance. Electrochemical reactions of the electrolyzer:

At the anode:



At the cathode:



Overall reaction:



5 Costs review. Data inputs

After establishing the foundations of the investment model, it is necessary to define the associated costs for each asset and the operational limitations that influence the system. Since money and time are closely linked, costs change over time due to factors like inflation, technological advancements, and market fluctuations. To ensure consistency, all costs must be expressed in terms of a specific reference year. The first assumption in this regard is that the project is set to begin in 2030. Therefore, all investment costs are considered in 2030 values, making 2030 the baseline (Year 0).

Most of the cost and technical data used in this study have been obtained from the Danish Energy Agency. Notably, some of the dataset were last updated in February 2025, which means that the values used in this report are based on data prior to such update. By ensuring that costs are framed consistently over time, this approach improves the reliability and comparability of investment projections.

5.1 Associated cost for each asset and technology specifics

For each asset, four types of costs have been included in the model[24]:

- **DEVEX** (Development Expenditure): Costs incurred during the early stages of a project, including feasibility studies, permitting, engineering, and project planning.
- **CAPEX** (Capital Expenditure): Initial investment costs for acquiring, upgrading, or constructing physical assets, such as equipment, infrastructure, and facilities.
- **OPEX** (Operational Expenditure): Recurring costs associated with the day-to-day operation and maintenance of a facility, including utilities, labor, and consumables.
- **ABEX** (Abandonment Expenditure): Costs related to decommissioning, dismantling, and site restoration at the end of a project's lifecycle.

Depending on the stage of the project, each cost has been considered: DEVEX and CAPEX were implemented in the early stages of the project. OPEX applies annually throughout the operation period. ABEX was considered after the final year of operation.

Finally DEVEX and ABEX are often unspecified in financial models. The Danish Energy Agency admits considering those values as a percentage of the CAPEX. Therefore, due to the lack of exact percentages an assumption had to be made[25]:

- DEVEX is estimated to be 20% of the total CAPEX.
- ABEX is assumed to be 10% of the total CAPEX.

Offshore windfarm

To start with, an offshore wind farm has been arbitrarily selected as the source of wind energy production, based on the assumption that it holds the most potential for future development. Therefore, according to the Danish Energy Agency[26], the associated costs have been determined based on three key factors:

- Turbine size: Larger turbines generally offer higher efficiency and lower costs per MW but require greater initial investments.
- Water depth: Deeper waters increase installation and maintenance costs due to the complexity of foundations and support structures.



- Distance to shore: Greater distances lead to higher transmission costs, affecting cabling, grid connection, and maintenance logistics. These factors are crucial in determining the final cost structure of the offshore wind farm and its impact on the overall investment model.

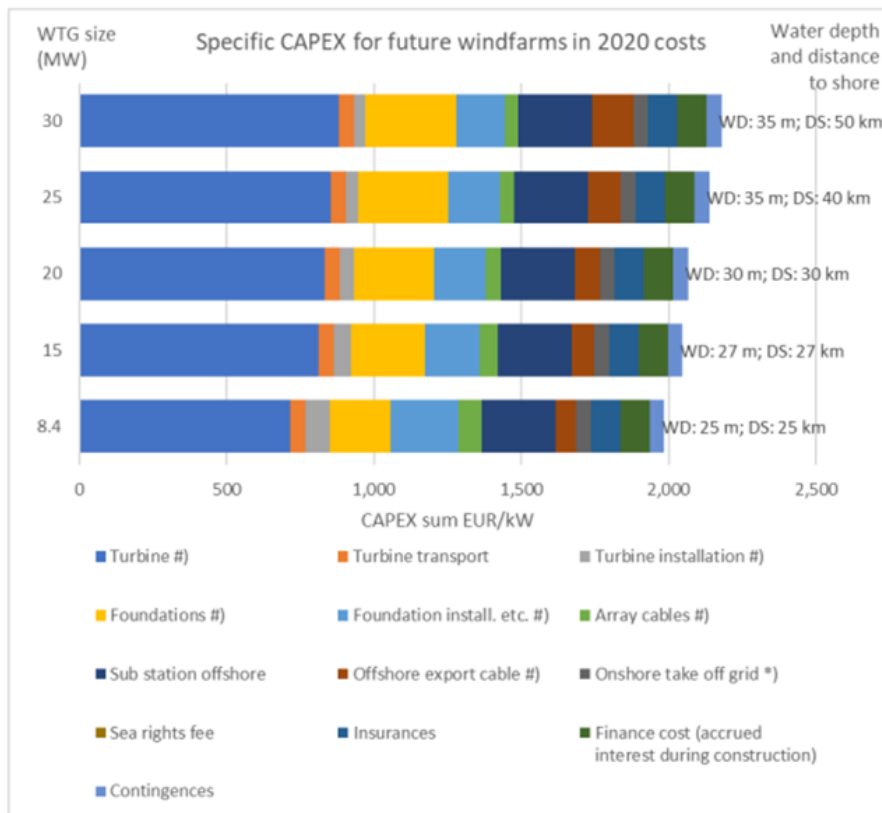


Figure 6: Detailed cost breakdown for future wind farms without learning rates

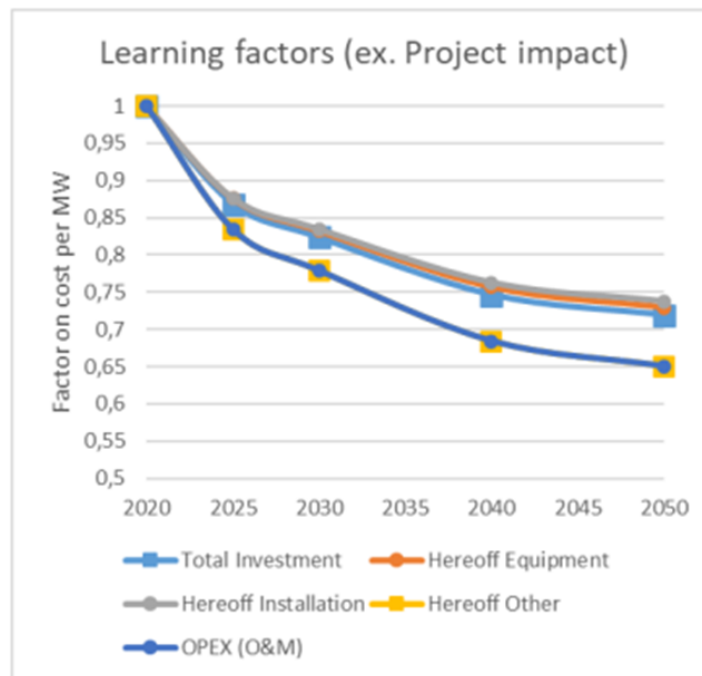


Figure 7: Learning rate-based cost reduction factors

For this study, a turbine size of 20 MW, a water depth of 30 meters, and a distance to shore of 30 km have been selected.

Generating capacity for one unit (MW)	20
Technical lifetime (years)	30
Planned outage (weeks/year)	0.5
Construction time (years)	2.5
Average annual full-load hours (MWh/MW)	4800
CAPEX (M€/MW)	1.8
OPEX (€/MW/year)	39,000
DEVEEX (M€/MW)	0.36
ABEX (M€/MW)	0.18

Table 2: Technical specification and cost details of the offshore windfarm

Photovoltaic solar farm

As for the PV panels, many different configurations could have been considered. The number of axes in the tracking system affects the capacity factor and therefore the full load hours. Additionally, panels can be monofacial or bifacial, with bifacial panels benefiting from reflection and scattered light, increasing the received irradiance. Due to the variety of configurations, a utility-scale, ground-mounted PV system has been selected. To maintain the actual cost of the panels, the full load hours have been preserved without adjusting for efficiency improvements. Furthermore, no land price has been considered, acknowledging the uncertainty this introduces. As a result, the values used in the study may be biased.

Generating capacity for one unit (MW)	40
Technical lifetime (years)	40
Planned outage (weeks/year)	0
Construction time (years)	0.5
Average annual full-load hours (MWh/MW)	1484
CAPEX (M€/MW)	0.38
OPEX (€/MW/year)	9,500
DEVEEX (M€/MW)	76,000
ABEX (M€/MW)	38,000

Table 3: Technical specification and cost details of the solar farm[26]

Electrolyzer AWE

Cost estimation and parameter inputs are based on both the Danish Energy Agency [27] and “Water electrolyzer operation scheduling for green hydrogen production”[23]. For the estimations, an AWE electrolyzer with a capacity of around 100 MW has been selected. “Internal Ramboll estimates yearly OPEX are 4 % for AEC”[27]. Technical and cost parameters are set forth below:



	CAPEX (€/kW)				
	2020	2025	2030	2040	2050
AEC	10 MW	1900	1400	875	675
	100 MW	1200	875	550	425
	1 GW	1100	800	500	400
					275

Figure 8: Table extracted from DEA: summary of all CAPEX values for AEC electrolyzers

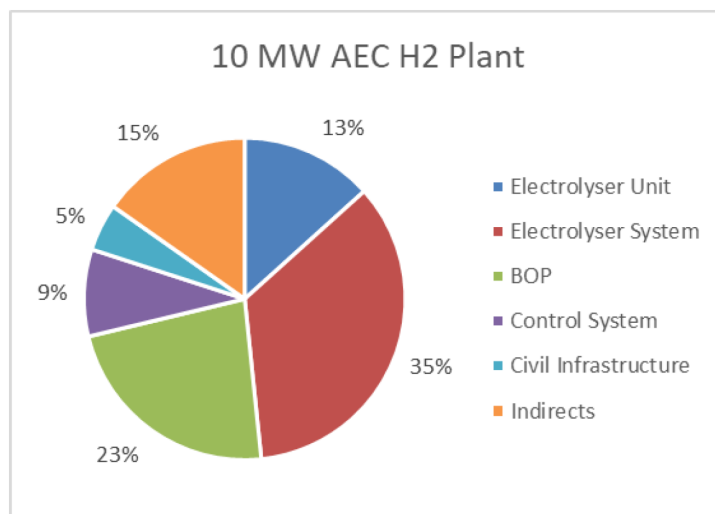


Figure 9: Cost distribution for AEC electrolyzers

Technical lifetime (years)	25 - 30
Planned outage (days/year)	11
Construction time (years)	2
Water consumption per 1 kg produced (kg)	15
Electricity consumption (KWh/kg-H ₂)	48.6
Frequency of stack replacement (h)	92,500
Ramp Up (%)	100*
Ramp Down (%)	100*
Minimum operation point (%)	15
CAPEX (M€/MW)	0.55
Stack replacement CAPEX (M€/MW)	0.115
OPEX (€/MW/year)	22,000
DEVEX (M€/MW)	110,000
ABEX (M€/MW)	55,000

Table 4: Technical specification and cost details of the electrolyzer[27]

* Note: ramp rate was defined as following: 0.17 %/s - 0.33%/s, which implies that along one hour, it can change 100% its operation point.

Reactor

The following table presents the financial data and characteristics of the reactor. It is important to note that the Danish Energy Agency[27] has grouped the financial parameters of both the reactor and distillation column under a single category. Therefore, both components are shown together in the same table. However, in the model implementation, these two assets must be treated separately. To achieve this, a cost division has been applied, assuming that the assets related to the distillation column accounts for 70% of the total cost of the reactor[28].

Generating capacity for one unit (TPD)	150
Technical lifetime (years)	30
Planned outage (weeks/year)	3
Construction time (years)	2
CO_2 input (ton/ton-MeOH)	1.4
H_2 input (ton/ton-MeOH)	0.19
Electricity consumption (MWh/ton-MeOH)	0.0014
Heat consumption (MWh/ton-MeOH)	0.0013
Ramp Up (%)	50
Ramp Down (%)	50
Minimum operation point (%)	20

Table 5: Technical specification for the reactor[8]

* **Note:** in the model, units have been converted from MW to tons per day (TPD) in order to make results more intuitive.

CAPEX (M€/TPD)*	0.25
OPEX (M€/(1,000 TPD/year)*	7
DEVEX (M€/TPD)*	0.05
ABEX (M€/TPD)*	0.025

Table 6: Financial parameters for both reactor and distillator.

Distillation column

As it has been mentioned above, financial parameters of the distillation column are shared with the reactor. In the following table the technological specifications of the distillator are being shown.



Generating capacity for one unit (TPD)	150
Technical lifetime (years)	30
Planned outage (weeks/year)	3
Construction time (years)	2
Pure MeOH input (ton-MeOH /ton)	1.565
Water output (ton/ton-MeOH)	0.550
Heat consumption (MWh/ton-MeOH)	0.002
Efficiency (%)	99.85
Ramp Up (%)	20
Ramp Down (%)	20
Minimum operation point (%)	20

Table 7: Technical specification for the distillation column

Battery

Batteries provide flexibility and versatility in the operation of the plant. Given that the system relies on variable renewable energy sources, batteries play a crucial role in balancing fluctuations, storing excess electricity during peak production and supplying it during periods of scarcity. However, scalability remains a key challenge for many battery technologies. Most commercially available options are power-intensive, meaning they can store large amounts of electricity but only for short durations. In contrast, this project requires an energy-intensive battery capable of ensuring stable operation over extended periods.

To meet these requirements, a sodium-sulfur (Na-S) battery has been selected. This technology offers high energy density and the ability to store electricity on the scale of hundreds of megawatt-hours, making it a suitable choice for long-duration energy storage in this application.

Energy storage capacity for one unit (MWh)	300
Output capacity for one unit (MW)	50
Input capacity for one unit (MW)	50
Technical lifetime (years)	24
Planned outage (days/year)	0
Construction time (years)	0.5
Round trip efficiency (%)	85
Minimum operation point (%)	10
Maximum operation point (%)	100
C rate	0.1667
CAPEX (M€/MW)	0.2446
OPEX (€/MW/year)	1.5
DEVEX (M€/MW)	44,900
ABEX (M€/MW)	22,450

Table 8: Technical specification and cost details of the battery[27]



Hydrogen storage

Hydrogen storage is known to be very expensive, primarily due to the cooling and compression processes, which significantly increase costs. While alternative storage methods, such as cavern storage, may offer a cheaper solution, they are not applicable for the current purpose.[27] For this study, seamless steel or aluminum tanks have been selected as the preferred storage option. These tanks are designed for stationary applications and offer the lowest average cost among the available hydrogen storage technologies, which makes them the most feasible option for this project.

Energy storage capacity for one unit (MWh)	16.7
Output capacity for one unit (MW)	-
Input capacity for one unit (MW)	0.09
Technical lifetime (years)	30
Planned outage (weeks/year)	2
Construction time (years)	0.4
Round trip efficiency (%)	88
Minimum operation point (%)	10
Maximum operation point (%)	100
C rate	0.05
CAPEX (€/kg)	500
OPEX (€/MW/year)	531.7*
DEVEX (€/kg)	100
ABEX (€/kg)	50

Table 9: Technical specification and cost details of the hydrogen storage[29]

Note: accounts for the compressor, which is assumed to be 100 kW.

CO₂ storage tank

As previously mentioned, the *CO₂* source for this project will be a CHP plant, which will supply a constant stream of carbon dioxide. However, since the plant's operation point can fluctuate, there may be instances of *CO₂* excess or scarcity. To address this variability, a storage solution is required to balance supply and demand.

For this purpose, pressurized tanks have been selected as an intermediate *CO₂* storage solution. Those tanks will allow the plant to store excess *CO₂* when supply exceeds demand and release it when needed, ensuring a stable and continuous methanol production process.



Energy storage capacity for one unit (m^3)	120
Technical lifetime (years)	25
Planned outage (weeks/year)	0
Construction time (years)	1.5
Round trip efficiency (%)	95
Minimum operation point (%)	5
Maximum operation point (%)	85
CAPEX (€/ton- CO_2)	3800
OPEX (€/ton- CO_2 /year)	114
DEVEX (€/ton- CO_2)	760
ABEX (€/ton- CO_2)	380

Table 10: Technical specification and cost details of the carbon dioxide storage[30]

Liquid raw and pure methanol storage

Due to the lack of specific cost data for methanol storage tanks, certain assumptions have been made to estimate their costs. The price of methanol tanks has been extrapolated from CO_2 tank costs, taking into account the following considerations:

- Methanol storage is simpler, as it remains in liquid form under ambient conditions, unlike CO_2 , which requires high-pressure or cryogenic storage.
- CO_2 tanks are more complex and expensive, given their need for pressure control and insulation, whereas methanol storage primarily focuses on fire safety measures.
- Methanol tanks require less specialized containment, making them cheaper to manufacture and maintain compared to CO_2 storage.

Hence, it has been estimated that the cost of methanol storage corresponds to 50% of the cost of CO_2 storage.

Energy storage capacity for one unit (m^3)	120
Technical lifetime (years)	25
Planned outage (weeks/year)	0
Construction time (years)	1.5
Round trip efficiency (%)	95
Minimum operation point (%)	5
Maximum operation point (%)	95
CAPEX (€/ton- $MeOH$)	1900
OPEX (€/ton- $MeOH$ /year)	57
DEVEX (€/ton- $MeOH$)	380
ABEX (€/ton- $MeOH$)	190

Table 11: Technical specification and cost details of methanol storages

Auxiliary equipment

Even though the investment costs for auxiliary equipment have been neglected, an additional cost associated with its energy consumption has been considered. This ensures that the operational impact of auxiliary systems is accounted for in the model, reflecting a more accurate estimation of total energy requirements and expenses.

Compressor To compress the syngas required for the reactor, an additional amount of energy is necessary. Specifically, for every ton of syngas, 0.144 MWh of electricity is required. That energy consumption has been accounted for in the model to ensure an accurate estimation of operational costs and energy requirements.

Desalinator AWE electrolyzers require pure water for hydrogen production. Purified water can be sourced from the sea and treated before use. To account for the energy required for desalination and purification, an additional energy demand of 0.02 MWh per cubic meter of water has been considered in the model.

Heater Finally, to maintain the operation of both the reactor and the distillation column, an additional heating demand is needed. To generate heat, the model assumes an efficiency of 110% for converting electricity into heat, reflecting the use of high-efficiency electrical heating systems.

5.2 Variable Renewable Energy

As previously mentioned, solar and wind profiles have been obtained from the webpage Renewables Ninja. To ensure consistency with the associated costs, the capacity factor and turbine properties have been carefully respected. Consequently, thirty years of historical data have been extracted, which are assumed to be representative of the next thirty years of production. For computational purposes, the processed data appears dimensionless. Thus, the actual electricity generation per hour is calculated as the installed capacity of the asset multiplied by the respective time series values. This approach allows for direct scaling of generation profiles based on the selected system capacities.

Wind generation

Offshore wind generation operates at 4,800 full load hours per year, which corresponds to a capacity factor of 0.548. The graph below represents the first year of data in per unit, providing insight into the hourly variation of wind power generation. For simplicity, only the first year is displayed, but it is important to note that all 30 years under consideration exhibit a similar capacity factor to the one stated, which indicates that the time follow similar trends across all years.

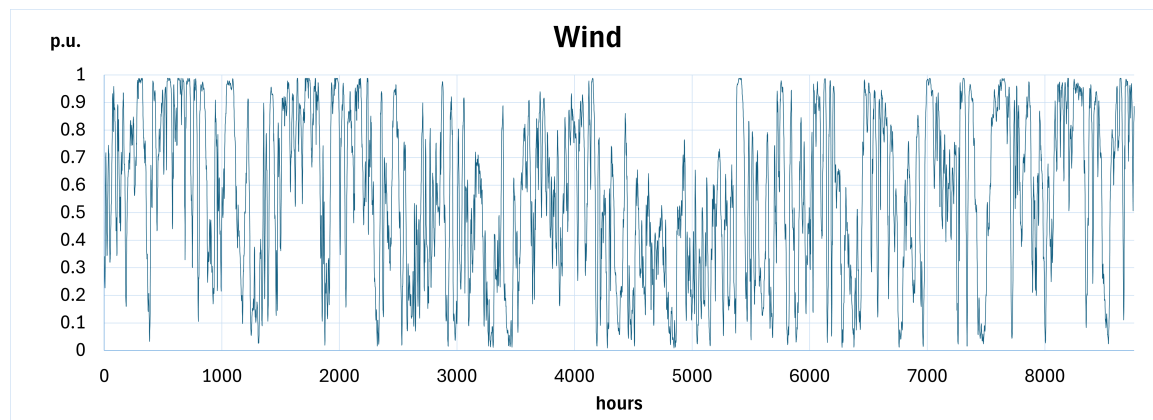


Figure 10: Time series of one year of offshore wind generation

Solar generation

On the other hand, we have the solar generation, which has 1484 of full load hours, which corresponds to a capacity factor of 0.169. Similar to wind power generation, only the first year is shown.

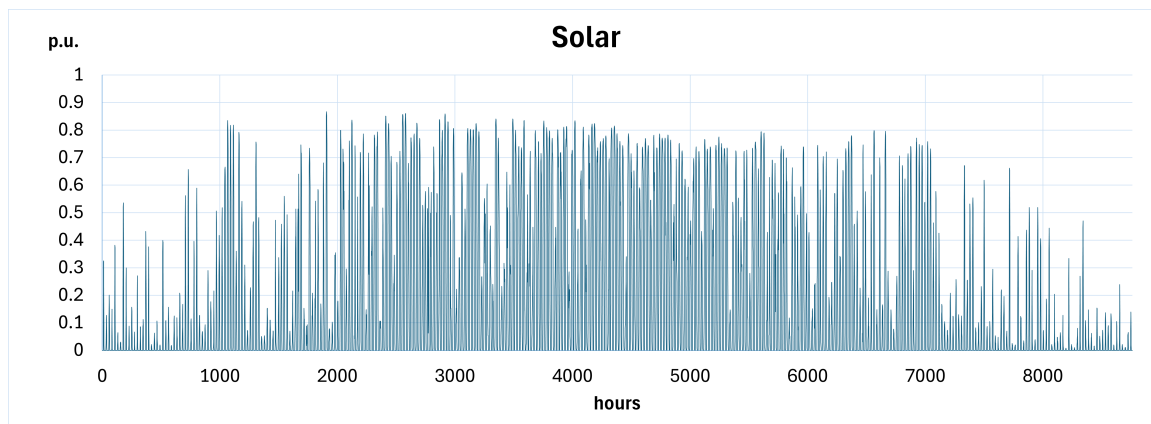


Figure 11: Time series of one year of photovoltaic solar generation

5.3 Electricity and CO₂ pricing

Electricity prices

To start with, it is important to stress that electricity prices play a crucial role in any investment model of this kind. Given their significant impact on project feasibility, a detailed study should ideally be conducted to obtain the most realistic results. However, due to time constraints, certain simplifications have been applied.

Thus, no correlation has been assumed between electricity generation and market prices, acknowledging the bias this introduces into the model. Instead, a steady-progressing time series with random noise has been generated to simulate realistic price fluctuations. Since electricity prices generally follow an upward trend driven by inflation, the chosen approach was to:

- Start with an average value
- Increase it annually based on the inflation rate,
- Introduce random noise to make the series more comparable to actual electricity price behavior.

The initial electricity price estimate was based on historical data from previous years. The first consideration was to use data from the last 10 years, which resulted in an average price of 65 €/MWh. However, this value was too outdated compared to the expected operation date of the project. A second approach was to use the last 5 years of data, but the inclusion of 2021 and 2022 (energy crisis years) led to unrealistically high values, with an average price of 97 €/MWh. To balance accuracy and realism, the final assumption was to take the average of 2023 and 2024, leading to an electricity price of 77 €/MWh as the base value.

Lastly, the inflation rate of Europe has been considered, as electricity markets across different countries are interconnected. The average annual inflation rate over the last 10 years is 2.1%[31], which has been applied to project future increases in electricity prices.

On the graphs below, there can be seen the difference between the synthetic time series generated and the actual electricity prices on years 2023 and 2024.

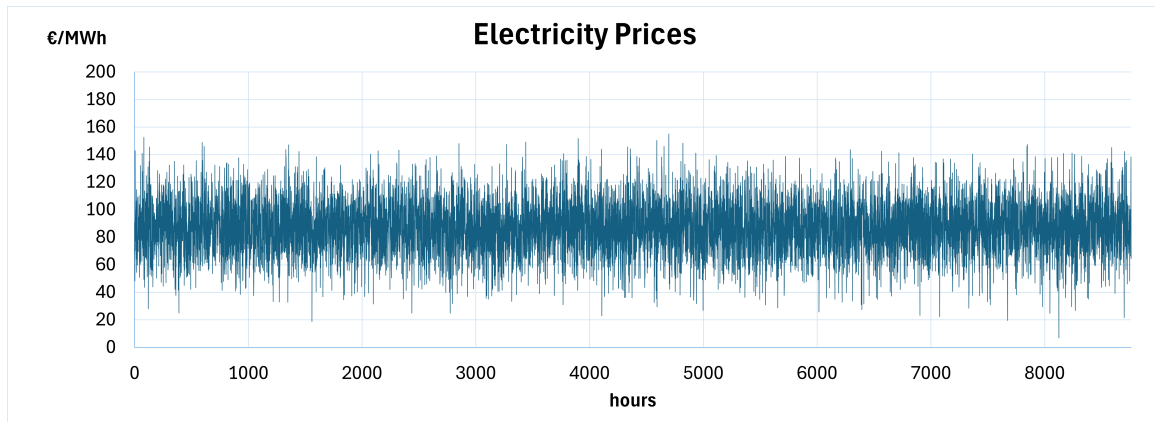


Figure 12: Time series of one year of electricity prices

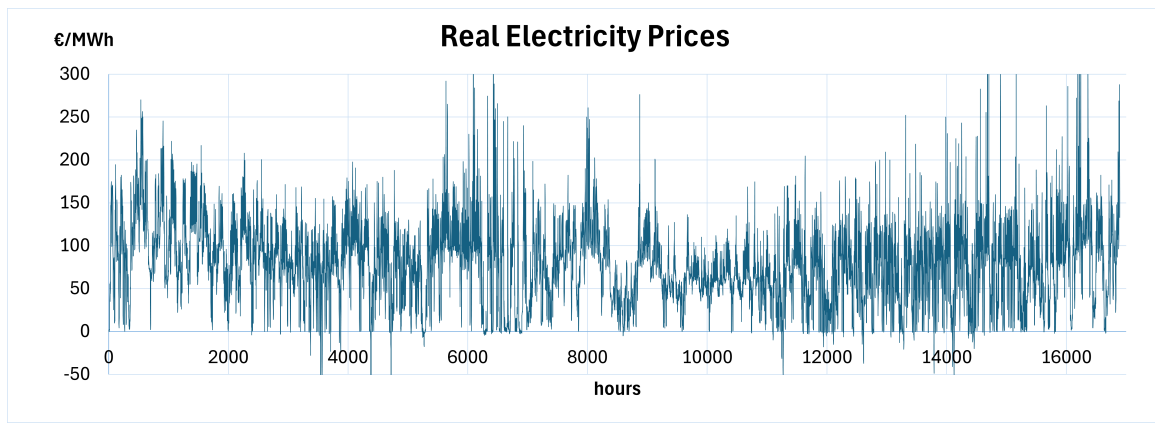


Figure 13: Time series of electricity prices in 2023 and 2024

CO₂ prices

The price of carbon dioxide has been assumed to remain constant throughout the entire operational period. Given the significant uncertainty surrounding future *CO₂* prices and the absence of a well-established market, a fixed price has been adopted to maintain consistency in cost estimation.

To align with reliable sources, the model uses the *CO₂* price proposed by the Danish Energy Agency, which is set at 100 €/ton. This assumption ensures that the economic evaluation remains transparent and comparable across different scenarios.

5.4 Financial parameters

Lastly, it is well known that assets and money depreciate over time. Therefore, it is necessary to annualize all costs to the point of the initial investment, referred to as Year Zero. Both investment costs and operational costs must be adjusted accordingly to ensure a consistent economic evaluation.

To perform this annualization, an investment rate is required. The value of this parameter can fluctuate depending on various factors, such as risk tolerance, financing conditions, and the expected profitability of the project.

Finally, the Danish Energy Agency applies a 4% discount rate for public projects, where financial risks are lower due to government backing. However, private projects face higher investment risks, including market fluctuations and financing costs. Therefore, using an 8% discount rate for this study is reasonable, as it better reflects the real cost of capital and aligns with industry practices for privately funded renewable energy projects.[32]

6 Model formulation. Decomposition techniques

The objective of the model is to minimize the total costs of the plant while ensuring a constant demand is met. The model operates on an hourly time step, meaning that all constraints and operational conditions must be satisfied at each hour. Electricity generation from variable renewable sources follows the time series data previously introduced. Additionally, the plant has the option to purchase electricity from the grid, though selling back to the grid is not permitted. Throughout the operational period, outputs can be stored, provided that all technical constraints related to storage assets are met. The key assets involved in methanol production, including the electrolyzer, reactor, and distillator, must comply with ramping constraints while operating within their respective capacity limits. At the end of the process, the constant demand is fulfilled.

The model incorporates four distinct scenarios that account for grid limitations and maintenance constraints, influencing both operational strategies and investment decisions. These scenarios are structured as two-by-two combinations, where the plant must undergo scheduled shutdown periods due to planned outages. Despite these interruptions, the total annual demand remains constant, meaning that during operational periods, the daily production rate must increase to compensate for downtime.

The second aspect of the scenarios involves the source of electricity. Initially, a fully connected grid without limitations was assumed, allowing the plant to operate seamlessly, even during dunkelflaute conditions—periods when neither wind nor solar power is available. However, the source of electricity also affects the classification of the produced methanol.

- If the plant draws electricity from the grid mix, which may include fossil fuel-based generation, the produced methanol cannot be fully labeled as green, as it has been mentioned above.
- On the other hand, by avoiding grid dependency and relying solely on renewable sources, the plant gains energy independence while ensuring that the methanol produced qualifies as green methanol.

During the initial formulation of this problem, various model configurations were evaluated, considering trade-offs between solution quality and computational cost. These configurations explored different levels of model complexity to balance accuracy and efficiency. Ultimately, an intermediate approach was chosen, allowing for a manageable computational burden while maintaining solution reliability. Additionally, the model was designed with the flexibility to incorporate decomposition techniques, enabling improved computational efficiency and facilitating future enhancements.

Different possibilities of models, deterministic one year, deterministic 30 years, stochastic with a large number of scenarios*:

	Solution complexity	Computational Cost
Deterministic with one year period	Low	Low
Deterministic with 30 years period	Medium	Medium
Stochastic model	High	High

Table 12: Comparison of model configurations

Note*: The number of scenarios in a stochastic model depends on its configuration and scope. If the model represents one year of operation, where each scenario introduces variations in that year, a dataset of around 50 different scenarios would be considered large. On the other hand, if the model operates over a 30-year period, where each scenario alters inputs across all years, then even as few as three scenarios would already represent a large-scale stochastic setup.



6.1 Mathematical model

Objective function

The objective function minimizes the total fixed and operational costs of the model, where discounted factors have been considered. Total costs correspond to all the expenditures such as CAPEX, fixed OPEX, ABEX and DEVEX. Alternatively, the variable costs considered have been the ones associated with the electricity imported from the grid and the costs of CO_2 .

$$\begin{aligned} \min_{\text{Capacities}_c, \text{Elec_grid}_t, \text{CO}_2, \text{imp}, t} & \left(\sum_{c=1}^C \text{Capacities}_c \cdot \text{Total_Costs}_c \right. \\ & \left. + \sum_{t=1}^T \text{Elec_grid}_t \cdot \text{El_price}_t + \sum_{t=1}^T \text{CO}_2, \text{imp}, t \cdot \text{CO}_2 \text{ price}_t \right) \end{aligned}$$

It is important to note that the terms Total_Costs_c , El_price_t and $\text{CO}_2 \text{ price}_t$ have already been annualized and discounted over the years. To do so, the expression of the Net Present Value have been implemented, where r accounts for the discount rate and t for the number of years:

$$NPV = \sum_{t=0}^n \frac{\text{Costs}_t}{(1+r)^t} \quad (6.1)$$

Constraints

Power Flow

This constraint enforces the energy balance, which ensures that the total energy consumption matches the available energy supply. It is worth mentioning that the model considers the possibility of energy curtail.

$$\text{VRE_elec}_t + \text{Elec_grid}_t + \text{Elec_from_batt}_t = \text{Elec_cons}_t + \text{Elec_to_batt}_t + \text{Elec_curt}_t \quad \forall t \in T$$

Maximum Capacities

Even if some assets can be easily scalable, like storage tanks, it is necessary to implement some physical limitations. Therefore, a maximum size for each asset has been implemented. It is worth mentioning that this constraint may help convergence, as it reduces the hull.

$$\text{Capacities}_c \leq \text{Max_Capacities}$$

Storage constraints

These constraints has been implemented for all five storages included in the model - battery included as it is a type of storage. In order to group all the constraints and make the writing more efficient, constraints have been grouped, as all the storages have to follow the mass conservation principle and C-rate considerations.

Boundary conditions With the aim of not oversize the assets, and also to avoid speculation with the stored products, an initial and equal state of charge had been established. This value corresponds to every storage to 50% of the maximum capacity. Equally, a final state of charge after 30 years of operation has been imposed.

$$SOC_{initial} = 0.5 \cdot Cap_{storage}$$

$$SOC_{final} \geq 0.5 \cdot Cap_{storage}$$



Operational limits For every storage, there are some operational limits that do not allow it to be fully charged or discharged. Therefore, these values have to be stated in the equations. It is worth mentioning that, depending on the type of storage, these operational limits may change.

$$SOC_t \leq MaxOperation \cdot Cap_{storage} \quad \forall t \in T$$

$$SOC_t \geq MinOperation \cdot Cap_{storage} \quad \forall t \in T$$

Mass balance - State of Charge (SOC) This constraint defines the dynamic mass balance of the storage system, ensuring that the stored quantity is continuously updated at each time step by balancing inflows, outflows, and efficiency losses. It maintains continuity in the storage system by accurately tracking storage levels over time, preventing discrepancies in mass or energy accounting. At each hourly interval, the storage updates its state by considering the amount entering and leaving, multiplied by efficiency factors that account for losses. Depending on the type of storage, the units vary; batteries are measured in megawatt-hours (MWh) to represent electrical energy storage, while hydrogen, CO_2 , and methanol storages are measured in tons, tracking the mass of stored material.

$$SOC_{t+1} = SOC_t + Chat \cdot eff_{in} - Dist \cdot eff_{out} \quad \forall t \in T$$

C-rate The C-rate for storages defines the rate at which a storage system can be charged or discharged relative to its total capacity. A 1C rate implies that the entire storage capacity is charged or discharged in one hour, while a 0.5C rate means that it takes two hours to fully charge or discharge.

$$Chat \leq Storage_Cap \cdot C\text{-rate} \quad \forall t \in T$$

$$Dist \leq Storage_Cap \cdot C\text{-rate} \quad \forall t \in T$$

Electrolyzer operation

The key aspects when modeling an electrolyzer's operation focus on ensuring its feasibility and efficiency. It is crucial to enforce operational limits, maintain adherence to ramp constraints, and guarantee that input and output requirements are met at every time step.

$$energy_elect_t \leq MaxOperation \cdot Cap_{electrolyzer} \quad \forall t \in T$$

$$energy_elect_t \geq MinOperation \cdot Cap_{electrolyzer} \quad \forall t \in T$$

$$H_2_output_t \cdot Elec_eff = energy_elect_t \quad \forall t \in T$$

$$H_2O_input_t \cdot H_2O_consumption = energy_elect_t \quad \forall t \in T$$

$$energy_elec_{t+1} - energy_elec_t \leq Cap_{electrolyzer} \cdot Ramp_Up \quad \forall t \in T$$

$$energy_elec_t - energy_elec_{t+1} \leq Cap_{electrolyzer} \cdot Ramp_Down \quad \forall t \in T$$

Reactor and Distillator operation

Similar to the electrolyzer, the reactor and distillator operate within their defined operational limits. Both units ensure mass and energy balance equations are maintained while adhering to ramping constraints to guarantee stable and efficient performance. For simplicity, only the reactor



equations are presented, as they share similar operational constraints and balance equations with the distillator.

$$MeOH_output_t \leq MaxOperation \cdot Cap_{reactor} \quad \forall t \in T$$

$$MeOH_output_t \geq MinOperation \cdot Cap_{reactor} \quad \forall t \in T$$

$$MeOH_output_t \cdot eff_{H_2} = mass_{H_2,reactor,t} + mass_{H_2,storage,t} \quad \forall t \in T$$

$$MeOH_output_t \cdot eff_{CO_2} = mass_{CO_2,stream,t} + mass_{CO_2,storage,t} \quad \forall t \in T$$

$$MeOH_output_t \cdot eff_{electricity} = electricity_{reactor,t} \quad \forall t \in T$$

$$MeOH_output_t \cdot eff_{heat} = heat_{reactor,t} \quad \forall t \in T$$

$$MeOH_output_{t+1} - MeOH_output_t \leq Cap_{reactor} \cdot Ramp_Up \quad \forall t \in T$$

$$MeOH_output_t - MeOH_output_{t+1} \leq Cap_{reactor} \cdot Ramp_Down \quad \forall t \in T$$

Demand fulfillment

Lastly, the meeting demand constraint ensures that a constant demand is met at every time step. This requirement drives investment in various assets, as the model must allocate resources to fulfill demand. Without this constraint, the optimal solution would result in zero asset investment.

$$Demand \leq MeOH_{discharged}$$

Additional constraints based on different scenarios

Grid limitation This constraint sets an upper limit on the amount of electricity that can be imported from the grid, ensuring that grid energy purchases remain within the defined capacity. In certain configurations mentioned earlier, this import limit is set to zero, effectively preventing any electricity extraction from the grid and enforcing complete reliance on variable renewable energy sources.

$$electricity_grid_t \leq Max_import, \quad \forall t \in T$$

Scheduled maintenance Every asset has specific planned outage periods, requiring a minimum number of shutdown days per year. To enhance efficiency, all planned outages are synchronized, with the total shutdown period determined by the asset with the longest outage requirement—in this case, the reactor, which has a planned outage of three weeks.

To model this shutdown period, an auxiliary binary variable was introduced, where 1 represents operational status and 0 represents a shutdown. Direct multiplication of these binary variables would introduce non-linearity into the model, which is best avoided. To maintain a linear formulation, additional auxiliary variables were introduced.

Since shutting down the electrolyzer, reactor, and distillator effectively shuts down the entire plant, only these assets are constrained. For simplicity, the electrolyzer's formulation is presented below.

The initial plan was to schedule the shutdown period during winter, when solar production is at its minimum. This approach aimed to minimize the impact on electricity availability. However, after running several simulations, the shutdown period was rescheduled to summer. Despite solar capacity peaking during this time, wind production, which contributes a larger share of total electricity generation, tends to have lower average output during summer months. As a result,



shifting the shutdown to this period allows for a better balance in overall energy availability while minimizing disruptions to the system.

$$m_t = \text{Maintenance}_{\text{period}}(\text{binary}) \quad \forall t \in T$$

$$z_{\text{elec},t} \leq \text{Cap}_{\text{electrolyzer}} \quad \forall t \in T$$

$$z_{\text{elec},t} \leq \text{MaxCap}_{\text{electrolyzer}} \cdot m \quad \forall t \in T$$

$$z_{\text{elec},t} \geq \text{Cap}_{\text{electrolyzer}} - (1 - m) \cdot \text{MaxCap}_{\text{electrolyzer}} \quad \forall t \in T$$

$$z_{\text{elec},t} \geq 0 \quad \forall t \in T$$

6.2 Decomposition techniques

The model is structured for a 30-year operational period, equivalent to 262,968 hours. Given the scale of the problem, decomposition techniques were initially considered to manage computational complexity. The core principle behind decomposition is to divide a large-scale problem into multiple smaller subproblems, hereby mitigating the curse of dimensionality. It is well established that computational requirements grow exponentially with problem size, making decomposition a valuable tool for improving solution feasibility and efficiency [33].

However, it is also important to highlight that the model was solvable without decomposition in its original form. Therefore, while not strictly necessary, decomposition was implemented primarily to facilitate further studies and benchmark results against alternative solution approaches. This allows for more flexible problem-solving methodologies and enhances the comparability of outcomes across different computational strategies.

Decomposition explanation

As previously mentioned, the goal of decomposition techniques is to break down a large-scale or complex problem into multiple smaller, more manageable subproblems. Through an iterative process, these subproblems are solved independently and provide feedback to a Master problem, which then updates the decision variables and refines the solution in subsequent iterations. For decomposition to be effective, the problem must exhibit a block-angular structure, ensuring that each subproblem can be solved independently without direct dependencies on other subproblems. However, many real-world problems do not naturally exhibit this structure, requiring modifications to eliminate interdependencies between subproblems. To achieve this, two decomposition techniques have been implemented:

- Benders' Decomposition: This method handles complicating variables, meaning it separates investment decisions (handled in the Master problem) from operational decisions (solved in the subproblems).
- Dantzig-Wolfe Decomposition: This approach manages complicating constraints, reformulating the problem so that each subproblem can be solved independently while ensuring feasibility through a column-generation process.

The main goal of combining these two techniques is to achieve a block-angular structure, allowing for efficient parallel computation of subproblems. By implementing these decomposition methods, the computational burden is significantly reduced, enabling the model to efficiently handle large-scale optimization over its 30-year horizon.



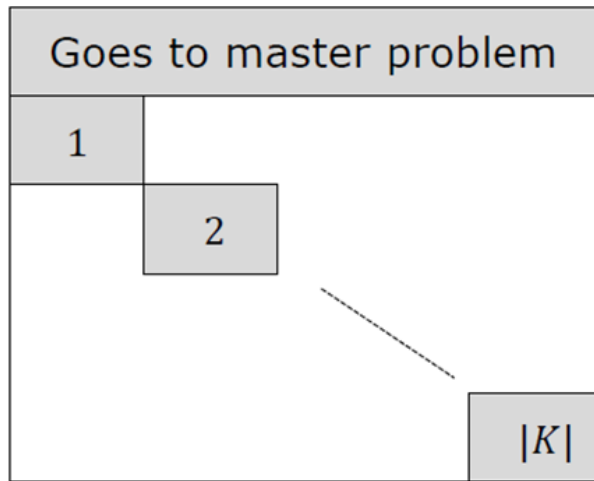


Figure 14: Block angular structure

Complicating variables

Complicating variables are those that appear in all subproblems, creating dependencies between them. In the present case, these variables correspond to asset sizes, such as the capacity of the electrolyzer, reactor, distillation column, and storage units. These variables are called complicating because their values remain fixed across all hours of operation, causing interdependencies that prevent the subproblems from being solved independently.

For instance, consider the size of the electrolyzer. If this variable were directly included in each subproblem, it would create a link between all time steps, requiring the subproblems to be solved as a single large problem. To eliminate this dependency and achieve decomposability, the asset size variables are moved to the Master problem, where they are optimized. In the subproblems, they remain as fixed parameters rather than decision variables, ensuring that each subproblem can be solved independently while still respecting the investment decisions made at the Master level.

$$\text{energy}_{\text{electrolyzer},h} \leq \text{Capacity}_{\text{electrolyzer}}, \quad \forall h \quad (6.2)$$

Complicating constraints

Similarly, complicating constraints also create interdependencies between subproblems, but in a different manner. Instead of linking subproblems through shared decision variables, these constraints connect time steps sequentially, forming a chain-like dependency that prevents independent resolution of each subproblem.

A key example of such a constraint is the mass balance equation for storage systems, which governs the state of charge (SOC) dynamics. This equation ensures that the stored quantity at each hour depends on the previous hour's state while accounting for inflows, outflows, and efficiency losses. Mathematically, it can be expressed as:

$$SOC_h = SOC_{h-1} + \eta_{in} \cdot \text{Inflow}_h - \eta_{out} \cdot \text{Outflow}_h, \quad \forall h \quad (6.3)$$

Because SOC is present in both hour h and $h - 1$, it links all subproblems across time, making them inseparable. To enable decomposition, these constraints are removed from the subproblems and handled by introducing auxiliary variables or relaxing constraints at the Master problem level. By doing so, each subproblem can be solved independently.

6.2.1 Benders

Benders decomposition relies on an iterative process using cutting planes to refine the solution of a large-scale problem. These cutting planes, generated by subproblems, add constraints to the Master problem, thereby improving the overall solution at each iteration. The subproblem also provides dual variables, which update dynamically in each iteration, guiding the Master problem towards optimality.

To implement this algorithm, the original optimization problem is divided into a Master problem and a subproblem. As previously defined, complicating variables — such as the size of assets — belong to the Master problem, while all other operational variables are part of the subproblem. However, at this stage, the subproblem remains indivisible because it still includes complicating constraints that create interdependencies.

The key role of the subproblem is to generate cutting planes, which iteratively enhance the solution of the Master problem. These cutting planes are derived from the dual problem, an optimization formulation obtained from the primal problem that seeks to maximize or minimize a bound on the primal solution using Lagrange multipliers.

Through iterative process, the Master problem determines investment decisions, such as asset sizes, and passes these values as parameters to the subproblem. The subproblem is then optimized under these fixed conditions, producing dual variables that are sent back to the Master problem in the form of a new cutting plane (constraint). Each iteration refines the feasible space of the Master problem. The algorithm concludes when the gap between the Master problem's objective value and the subproblem's objective value reaches a specified threshold, ensuring convergence to an optimal solution.

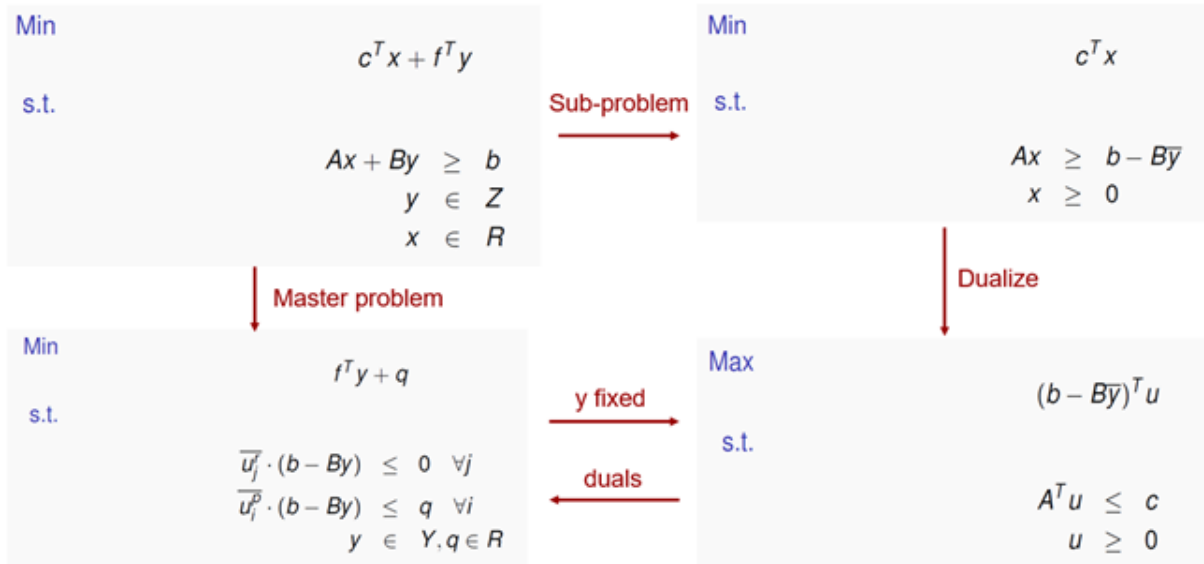


Figure 15: Benders algorithm scheme

Finally, it is important to highlight an additional consideration. In some cases, the solution provided by the Master problem may lead to an unbounded subproblem, meaning that the subproblem fails to find a feasible solution. When this occurs, instead of solving the subproblem in its original form, a ray problem is formulated and solved.

The ray problem differs from the standard subproblem in that its right-hand side constraints are set to zero, effectively identifying infeasibilities rather than optimizing for an objective function. Instead of generating an optimality cut, the ray problem produces a feasibility cut, which is then

added to the Master problem. This feasibility cut ensures that future iterations of the Master problem avoid selecting solutions that would lead to infeasibility in the subproblem.

For simplification, the detailed formulation of the subproblem has been omitted, but it is important to note that the feasibility cut is a key component in ensuring convergence and feasibility within the Benders' decomposition algorithm.

Model formulation

In order to implement the algorithm, two main models have been added - three if ray problem is considered.

Master problem

Objective function

The objective function accounts for the cost of every asset plus the q value that comes from the subproblem. q is an auxiliary variable that englobes all the variable costs and composes the cutting planes.

$$\min \quad Capacities_c \cdot \text{Total_Costs}_c + q \quad (6.4)$$

Constraints

This first constraint enforces maximum capacities for the assets.

$$Capacities_c \leq maxCapacities, \quad \forall c \quad (6.5)$$

The constraint below ensures that the recourse variable q captures the system feasibility, incorporating storage dynamics, demand balance, ramping constraints, and overall operational feasibility. Within this constraint, all terms except p_{cap} , which represents the asset capacities, are treated as fixed parameters.

Since p_{cap} is a decision variable in the Master problem, each iteration refines its value, leading to a progressively constrained feasible space. As the solution evolves, newly generated asset capacities become increasingly restricted, improving the overall optimality of the solution.

$$\begin{aligned} q \geq & \sum_t \left[p_{flow} \cdot (Wind \cdot p_{cap,0} + Solar \cdot p_{cap,1}) - max_grid \cdot grid_max \right. \\ & + init_{bat} \cdot p_{cap,5} \cdot Battery_{init} + fin_{bat} \cdot p_{cap,5} \cdot Battery_{final} \\ & + bat_{min} \cdot p_{cap,5} \cdot Battery_{min} - bat_{max} \cdot p_{cap,5} \cdot Battery_{max} \\ & - C_{bat,1} \cdot p_{cap,5} \cdot Battery_C - C_{bat,2} \cdot p_{cap,5} \cdot Battery_C \\ & - elec_{max} \cdot p_{cap,2} + elec_{min} \cdot p_{cap,2} \cdot opelec,min \\ & - elec_{ramp,up} \cdot p_{cap,2} \cdot opelec,ramp,up - elec_{ramp,down} \cdot p_{cap,2} \cdot opelec,ramp,down \\ & + balance \cdot Demand + init_{h2} \cdot p_{cap,6} \cdot H2_{init} + fin_{h2} \cdot p_{cap,6} \cdot H2_{final} \\ & + h2_{min} \cdot p_{cap,6} \cdot H2_{min} - h2_{max} \cdot p_{cap,6} \cdot H2_{max} \\ & - C_{rate,h2,1} \cdot p_{cap,6} \cdot H2_C - C_{rate,h2,2} \cdot p_{cap,6} \cdot H2_C \\ & - reac_{max} \cdot p_{cap,3} + reac_{min} \cdot p_{cap,3} \cdot opreac,min \\ & - reac_{ramp,up} \cdot p_{cap,3} \cdot opreac,ramp,up - reac_{ramp,down} \cdot p_{cap,3} \cdot opreac,ramp,down \\ & - dest_{max} \cdot p_{cap,4} + dest_{min} \cdot p_{cap,4} \cdot opdest,min \\ & - dest_{ramp,up} \cdot p_{cap,4} \cdot opdest,ramp,up - dest_{ramp,down} \cdot p_{cap,4} \cdot opdest,ramp,down \\ & + init_{MeOH,sto} \cdot p_{cap,7} \cdot MeOH_{init} + fin_{MeOH,sto} \cdot p_{cap,7} \cdot MeOH_{final} \\ & \left. + MeOH_{min} \cdot p_{cap,7} \cdot MeOH_{min} - MeOH_{max} \cdot p_{cap,7} \cdot MeOH_{max} \right], \quad \forall t \end{aligned} \quad (6.6)$$



Sub problem

In the dual problem the constraints become variables and vice versa. The right hand side of the original problem becomes part of the dual objective function.

Objective Function The objective function is formulated as:

$$\begin{aligned}
 \max \quad q = & \sum_h p_{\text{flow},h} \cdot (\text{Wind} \cdot P_{\text{cap},0} + \text{Solar} \cdot P_{\text{cap},1}) \\
 & - \sum_h (\text{max_grid} \cdot \text{grid_max}) \\
 & + \text{init_bat} \cdot P_{\text{cap},5} \cdot \text{Battery}_2 + \text{fin_bat} \cdot P_{\text{cap},5} \cdot \text{Battery}_3 \\
 & + \sum_h [\text{bat_min} \cdot P_{\text{cap},5} \cdot \text{Battery}_4 - \text{bat_max} \cdot P_{\text{cap},5} \cdot \text{Battery}_5 \\
 & \quad - C_{\text{bat_1}} \cdot P_{\text{cap},5} \cdot \text{Battery}_6 - C_{\text{bat_2}} \cdot P_{\text{cap},5} \cdot \text{Battery}_6] \\
 & + \sum_h [-\text{elec_max} \cdot P_{\text{cap},2} + \text{elec_min} \cdot P_{\text{cap},2} \cdot \text{op_elec}_2 \\
 & \quad - \text{elec_ramp_up} \cdot P_{\text{cap},2} \cdot \text{op_elec}_0 - \text{elec_ramp_down} \cdot P_{\text{cap},2} \cdot \text{op_elec}_1] \\
 & + \sum_h \text{balance} \cdot \text{Demand} \\
 & + \text{init_h2} \cdot P_{\text{cap},6} \cdot \text{H2storage}_2 + \text{fin_h2} \cdot P_{\text{cap},6} \cdot \text{H2storage}_3 \\
 & + \sum_h [\text{h2_min} \cdot P_{\text{cap},6} \cdot \text{H2storage}_4 - \text{h2_max} \cdot P_{\text{cap},6} \cdot \text{H2storage}_5 \\
 & \quad - C_{\text{rate_h2_1}} \cdot P_{\text{cap},6} \cdot \text{H2storage}_6 - C_{\text{rate_h2_2}} \cdot P_{\text{cap},6} \cdot \text{H2storage}_6] \\
 & + \text{init_CO2} \cdot P_{\text{cap},8} \cdot \text{CO2storage}_2 + \text{fin_CO2} \cdot P_{\text{cap},8} \cdot \text{CO2storage}_3 \\
 & + \sum_h [\text{CO2_min} \cdot P_{\text{cap},8} \cdot \text{CO2storage}_4 - \text{CO2_max} \cdot P_{\text{cap},8} \cdot \text{CO2storage}_5 \\
 & \quad + \text{CO2_str_min} \cdot \text{CO2storage}_6 - \text{CO2_str_max} \cdot \text{CO2storage}_7] \\
 & + \sum_h [-\text{reac_max} \cdot P_{\text{cap},3} + \text{reac_min} \cdot P_{\text{cap},3} \cdot \text{op_reac}_2 \\
 & \quad - \text{Reac_ramp_up} \cdot P_{\text{cap},3} \cdot \text{op_reac}_0 - \text{Reac_ramp_down} \cdot P_{\text{cap},3} \cdot \text{op_reac}_1] \\
 & + \text{init_MeOH_sto} \cdot P_{\text{cap},7} \cdot \text{raw_MeOH_sto}_2 + \text{fin_MeOH_sto} \cdot P_{\text{cap},7} \cdot \text{raw_MeOH_sto}_3 \\
 & + \sum_h [\text{raw_MeOH_min} \cdot P_{\text{cap},7} \cdot \text{raw_MeOH_sto}_4 \\
 & \quad - \text{raw_MeOH_max} \cdot P_{\text{cap},7} \cdot \text{raw_MeOH_sto}_5] \\
 & + \sum_h [-\text{dest_max} \cdot P_{\text{cap},4} + \text{dest_min} \cdot P_{\text{cap},4} \cdot \text{op_dest}_2 \\
 & \quad - \text{dest_ramp_up} \cdot P_{\text{cap},4} \cdot \text{op_dest}_0 - \text{dest_ramp_down} \cdot P_{\text{cap},4} \cdot \text{op_dest}_1] \\
 & + \text{init_pure} \cdot P_{\text{cap},9} \cdot \text{Pure_MeOH_sto}_2 + \text{fin_pure} \cdot P_{\text{cap},9} \cdot \text{Pure_MeOH_sto}_3 \\
 & + \sum_h [\text{MeOH_min} \cdot P_{\text{cap},9} \cdot \text{Pure_MeOH_sto}_4 \\
 & \quad - \text{MeOH_max} \cdot P_{\text{cap},9} \cdot \text{Pure_MeOH_sto}_5]
 \end{aligned} \tag{6.7}$$

Constraints The following constraints define the dual problem of the original formulation, where the original variables now appear within the constraints. The right-hand side of the subproblem consists of elements from the original objective function, specifically electricity prices and CO_2 prices. Since the equations have been previously detailed, only the dual formulation is presented without further explanation.

$$-p_{\text{flow}} - \text{max_grid} \leq \text{Prices} \quad (\text{Electricity Purchase}) \quad (6.8)$$

$$p_{\text{flow}} \leq 0 \quad (\text{Electricity Sell Constraint}) \quad (6.9)$$

$$\text{init}_{\text{bat}} - \text{bat}_{\text{sto},0} + \text{bat}_{\text{min},0} - \text{bat}_{\text{max},0} \leq 0 \quad (\text{Battery SOC at } t = 0) \quad (6.10)$$

$$\text{bat}_{\text{sto},t} - \text{bat}_{\text{sto},t+1} + \text{bat}_{\text{min},t+1} - \text{bat}_{\text{max},t+1} \leq 0 \quad (\text{Battery SOC Balance}) \quad (6.11)$$

$$-\text{bat}_{\text{sto},t} \cdot \eta_{\text{bat}} + p_{\text{flow},t} - C_{\text{bat},1,t} \leq 0 \quad (\text{Battery Charging Limit}) \quad (6.12)$$

$$\text{bat}_{\text{sto},t} / \eta_{\text{bat}} - p_{\text{flow},t} - C_{\text{bat},2,t} \leq 0 \quad (\text{Battery Discharging Limit}) \quad (6.13)$$

$$p_{\text{flow},t} - \text{elec}_{\text{max},t} + \text{elec}_{\text{min},t} - \text{elec}_{\text{op},t} - \text{elec}_{\text{ramp-up},t-1} + \text{elec}_{\text{ramp-down},t-1} \leq 0 \quad (\text{Electrolyzer Operation}) \quad (6.14)$$

$$\text{elec}_{\text{op},t} \cdot \eta_{\text{elec}} + \text{compressor}_{H_2,t} \leq 0 \quad (\text{Hydrogen Production from Electrolyzer}) \quad (6.15)$$

$$\text{init}_{H_2} - \text{h2}_{\text{sto},0} + \text{h2}_{\text{min},0} - \text{h2}_{\text{max},0} \leq 0 \quad (\text{Initial Hydrogen Storage}) \quad (6.16)$$

$$\text{h2}_{\text{sto},t} - \text{h2}_{\text{sto},t+1} + \text{h2}_{\text{min},t+1} - \text{h2}_{\text{max},t+1} \leq 0 \quad (\text{Hydrogen Storage Balance}) \quad (6.17)$$

$$-\text{h2}_{\text{sto},t} \cdot \eta_{H_2} - C_{\text{rate},H_2,1,t} - \text{compressor}_{H_2,t} \leq 0 \quad (\text{Hydrogen Charging Constraint}) \quad (6.18)$$

$$\text{h2}_{\text{sto},t} / \eta_{H_2} - C_{\text{rate},H_2,2,t} - \text{reac}_{H_2,t} \leq 0 \quad (\text{Hydrogen Discharging Constraint}) \quad (6.19)$$

$$\text{init}_{CO_2} - CO_2_{\text{sto},0} + CO_2_{\text{min},0} - CO_2_{\text{max},0} \leq 0 \quad (\text{Initial CO}_2 \text{ Storage}) \quad (6.20)$$

$$CO_2_{\text{sto},t} - CO_2_{\text{sto},t+1} + CO_2_{\text{min},t+1} - CO_2_{\text{max},t+1} \leq 0 \quad (\text{CO}_2 \text{ Storage Balance}) \quad (6.21)$$

$$CO_2_{\text{str,min}} - CO_2_{\text{str,max}} + CO_2_{\text{comp},t} \leq CO_2 \text{ Prices} \quad (\text{CO}_2 \text{ Purchase Constraint}) \quad (6.22)$$

$$-\text{compressor}_{H_2,t} - \text{reac}_{H_2,t} \leq 0 \quad (\text{Hydrogen Input to Reactor}) \quad (6.23)$$

$$-CO_2_{\text{comp},t} - \text{reac}_{CO_2,t} \leq 0 \quad (\text{CO}_2 \text{ Input to Reactor}) \quad (6.24)$$

$$-\text{reac}_{\text{max},t} + \text{reac}_{\text{min},t} + \text{reac}_{H_2,t} \cdot \alpha + \text{reac}_{CO_2,t} \cdot \beta \leq 0 \quad (\text{Reactor Operation Constraint}) \quad (6.25)$$



$$\text{init}_{\text{MeOH}} - \text{MeOH}_{\text{sto},0} + \text{MeOH}_{\text{min},0} - \text{MeOH}_{\text{max},0} \leq 0 \quad (\text{Initial Methanol Storage}) \quad (6.26)$$

$$-\text{MeOH}_{\text{sto},t+1} + \text{MeOH}_{\text{sto},t} + \text{MeOH}_{\text{min},t+1} - \text{MeOH}_{\text{max},t+1} \leq 0 \quad (\text{Methanol Storage Balance}) \quad (6.27)$$

$$-\text{compr}_{\text{MeOH},t} - \text{dest}_{\text{rawMeOH},t} \leq 0 \quad (\text{Methanol Processing}) \quad (6.28)$$

$$-\text{dest}_{\text{max},t} + \text{dest}_{\text{min},t} + \text{dest}_{\text{rawMeOH},t} \cdot \eta_{\text{dest}} \leq 0 \quad (\text{Methanol Distillation Constraint}) \quad (6.29)$$

6.2.2 Dantzig-Wolfe

Once the first decomposition method is implemented, the second one can be applied. The starting point is the subproblem obtained from the first decomposition algorithm, which has already eliminated complicating variables. By further removing the complicating constraints, the resulting subproblem can be fully decomposed into multiple independent subproblems. This transformation would allow for a more efficient solution process, maximizing the computational benefits of decomposition techniques.

The Dantzig-Wolfe algorithm relies on the Minkowski-Weyl Theorem and column generation.

- The Minkowski-Weyl theorem states that any point within a convex polyhedron can be expressed as a combination of its extreme points. This principle allows feasible solutions to be represented in terms of a limited set of key points rather than handling the entire problem at once.
- Column generation is an iterative optimization technique that starts with a restricted set of decision variables and dynamically introduces new ones that improve the objective function. These new variables are identified by solving a subproblem, known as the pricing problem based on the minimum reduced cost, which finds the most promising column to be added. The master problem is then re-optimized until no further improvement can be made.

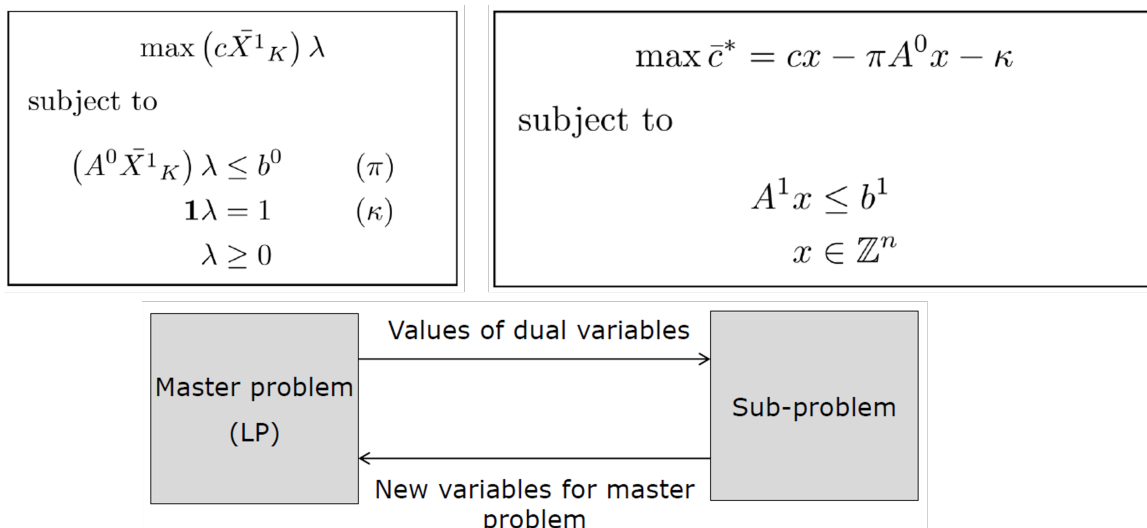


Figure 16: Dantzig-Wolfe algorithm scheme

The initial approach for implementing the Dantzig-Wolfe decomposition was to create a subproblem for each hour of operation. However, this proved to be highly inefficient, as the computational overhead of managing such a vast number of subproblems outweighed the benefits of decomposition. Given that the model processes over 250,000 hours, even if each subproblem took just 0.01 seconds to solve, the total runtime would still be excessively long. To address this, the problem was instead divided into segments of 1,000 hours. This adjustment significantly reduced the number of subproblems while maintaining fast solution times for each, striking a balance between efficiency and computational feasibility.

Model formulation

Unlike the Benders algorithm, the Dantzig-Wolfe decomposition does not require dualizing* the problem but instead divides the problem and strategically assigns constraints to either the master problem or the subproblems. In this case, as previously mentioned, complicating constraints—such as mass balance equations and ramping constraints for the methanol production assets—are handled within the master problem, while the subproblems are solved independently. By removing these constraints, subproblems are grouped and solved in 1000-hour intervals, feeding their solutions back to the master problem. The termination condition of the algorithm is based on column generation and the minimum reduced cost criterion, meaning that the process stops when the objective value of the subproblem reaches zero (or a near-zero threshold), indicating that no further columns need to be generated. This ensures computational efficiency while still achieving optimality.

Note: as it can be seen in 16, the model extract the dual variables π and κ from the Master problem, but this does not mean that the problem has been dualized.

Master problem

The master problem incorporates a term λ that accounts for the solutions retrieved from the subproblems.

Objective function

The objective function has already been defined in the previous subproblem. The only term that implements this time is the element λ , which represents the combination of solutions extracted from the subproblem.

$$\max \quad \sum_k \lambda_k \cdot q_k \quad (6.30)$$

Constraints

Lambda

$$\sum_k \lambda_k = 1 \quad (6.31)$$

Battery State of Charge Constraints

$$\sum_k \lambda_k \left(\text{SOC}_{\text{bat},t-1}^k - \text{SOC}_{\text{bat},t}^k + \text{bat}_{\min,t}^k - \text{bat}_{\max,t}^k \right) \leq 0, \quad \forall t = 1000, 2000, \dots, T \quad (6.32)$$



Electrolyzer Operational Constraints

$$\sum_k \lambda_k \left(p_{\text{flow},t}^k - \max_{\text{elec},t}^k + \min_{\text{elec},t}^k - \text{elec}_{\text{op},t}^k - \text{elec}_{\text{ramp-up},t-1}^k + \text{elec}_{\text{ramp-down},t-1}^k + \text{elec}_{\text{ramp-up},t}^k - \text{elec}_{\text{ramp-down},t}^k \right) \leq 0, \quad \forall t = 1000, 2000, \dots, T \quad (6.33)$$

Hydrogen Storage Balance Constraints

$$\sum_k \lambda_k \left(\text{SOC}_{\text{H}_2,t-1}^k - \text{SOC}_{\text{H}_2,t}^k + \text{H}_2_{\text{min},t}^k - \text{H}_2_{\text{max},t}^k \right) \leq 0, \quad \forall t = 1000, 2000, \dots, T \quad (6.34)$$

CO Storage Balance Constraints

$$\sum_k \lambda_k \left(\text{SOC}_{\text{CO}_2,t-1}^k - \text{SOC}_{\text{CO}_2,t}^k + \text{CO}_2_{\text{min},t}^k - \text{CO}_2_{\text{max},t}^k \right) \leq 0, \quad \forall t = 1000, 2000, \dots, T \quad (6.35)$$

Methanol Reactor Constraints

$$\begin{aligned} \sum_k \lambda_k \left(- \max_{\text{reac},t}^k + \min_{\text{reac},t}^k + H_2_{\text{reac},t}^k + CO_2_{\text{reac},t}^k + E_{\text{reac},t}^k + Q_{\text{reac},t}^k \right. \\ \left. - \text{Reac}_{\text{ramp-up},t-1}^k + \text{Reac}_{\text{ramp-down},t-1}^k + \text{Reac}_{\text{ramp-up},t}^k \right. \\ \left. - \text{Reac}_{\text{ramp-down},t}^k + \text{compr}_{\text{MeOH},t}^k \right) \leq 0, \quad \forall t = 1000, 2000, \dots, T \end{aligned} \quad (6.36)$$

Raw Methanol Storage Balance Constraints

$$\begin{aligned} \sum_k \lambda_k \left(\text{SOC}_{\text{rawMeOH},t-1}^k - \text{SOC}_{\text{rawMeOH},t}^k \right. \\ \left. + \text{rawMeOH}_{\text{min},t}^k - \text{rawMeOH}_{\text{max},t}^k \right) \leq 0, \quad \forall t = 1000, 2000, \dots, T \end{aligned} \quad (6.37)$$

Methanol Distillation Constraints

$$\begin{aligned} \sum_k \lambda_k \left(- \max_{\text{dist},t}^k + \min_{\text{dist},t}^k + \text{rawMeOH}_{\text{dist},t}^k \cdot \eta + H_2O_{\text{dist},t}^k + Q_{\text{dist},t}^k \cdot \theta + \text{SOC}_{\text{dist},t}^k \right. \\ \left. - \text{dist}_{\text{ramp-up},t-1}^k + \text{dist}_{\text{ramp-down},t-1}^k + \text{dist}_{\text{ramp-up},t}^k - \text{dist}_{\text{ramp-down},t}^k \right) \leq 0, \quad \forall t = 1000, 2000, \dots, T \end{aligned} \quad (6.38)$$

Pure Methanol Storage Balance Constraints

$$\sum_k \lambda_k \left(\text{SOC}_{\text{MeOH},t-1}^k - \text{SOC}_{\text{MeOH},t}^k + \text{MeOH}_{\text{min},t}^k - \text{MeOH}_{\text{max},t}^k \right) \leq 0, \quad \forall t = 1000, 2000, \dots, T \quad (6.39)$$

Sub problem

To sum up, the remaining subproblems retain all the equations from the original subproblem but the ones defined in the master problem. However, since they are no longer linked by complicating constraints, each subproblem can now be solved independently, significantly reducing computational complexity.



7 Results

The results are based on the two model configurations, each defined by the possibility of importing electricity from the grid. Additionally, given the large-scale nature of the model, computational time is a critical factor. Consequently, a dedicated analysis on computational performance has been carried out. Lastly, since decomposition techniques have been implemented, their effectiveness and impact on performance have also been assessed.

7.1 Output production and operation of the plant

To start with, it is important to emphasize that the plant operates for a total of thirty years. However, for practical reasons, only the first year of operation is presented, as it exhibits similarities with the subsequent years. Nonetheless, it is essential to note that simulating thirty independent years instead of a single repeated year with typical weather data would yield different results. This is primarily because storage systems would not have the ability to regulate across multiple years, and the plant would not be able to compensate for fluctuations in renewable energy input using the same asset sizing.

Since a maintenance schedule is incorporated into the model, it can be observed that the plant shuts down approximately between hour 4500 and 5000. This is a cyclical condition, meaning that every year, the plant is forced to shut down during this period.

Model configuration with grid connection

The first three plots represent the outputs of assets directly involved in methanol production. At first sight, the graphs may appear almost identical, but they differ in the variation of their operational points. As a reminder, the ramp rates of the electrolyzer, reactor, and distillation column are 100%, 50%, and 20% per hour, respectively. Therefore, it can be seen that the electrolyzer and reactor frequently adjust their operational points, while the distillation column remains relatively stable.

Another key reason for this variability is that both the electrolyzer and the reactor are influenced by renewable energy production, whereas the distillation column is not. Although all these assets have storage systems before their operation, only raw methanol storage provides enough buffering capacity to stabilize the distillation column's operation point. In contrast, battery and hydrogen storage do not have sufficient capacity to fully stabilize the operation of the electrolyzer and reactor. In theory, grid electricity could provide a stable energy supply, reducing the variability in operational points. However, as will be explained further, relying on the grid would significantly increase costs, making it an economically unfavorable option.

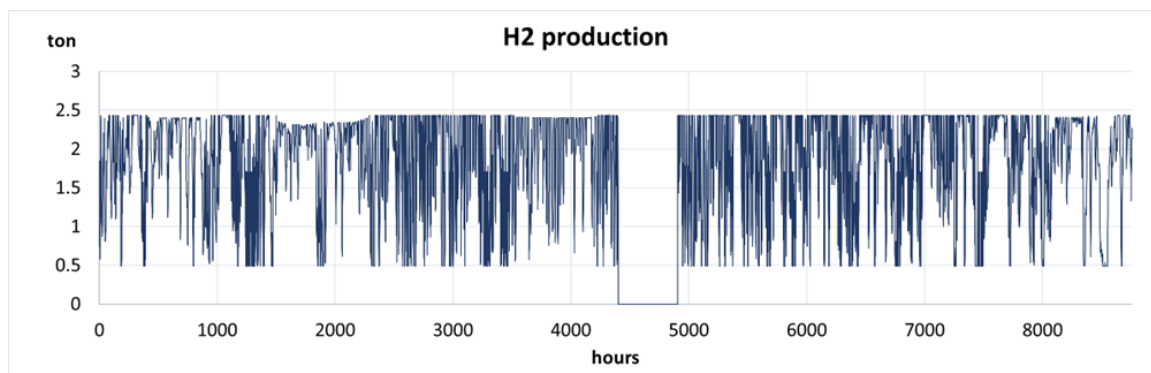


Figure 17: First year of hourly hydrogen production with grid connection

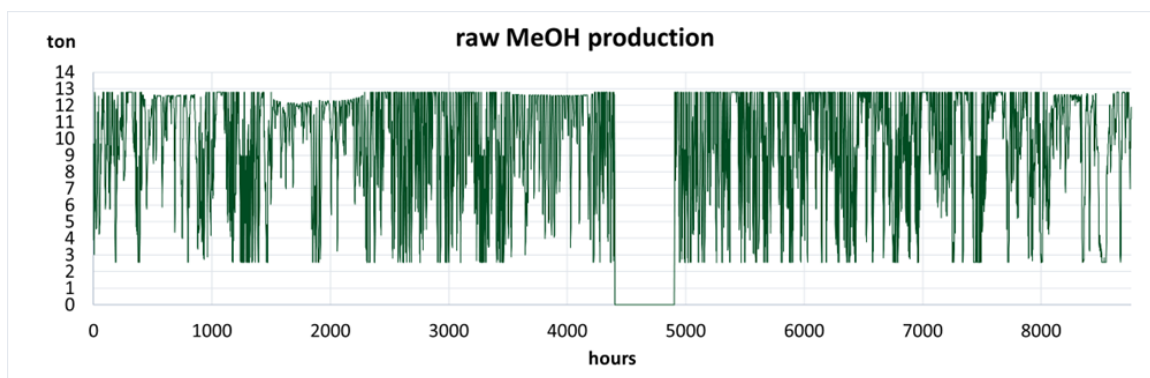


Figure 18: First year of hourly raw methanol production

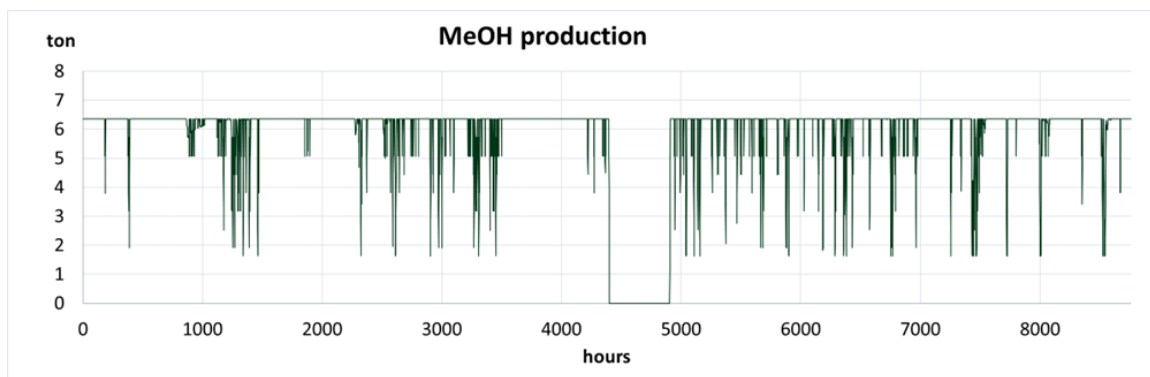


Figure 19: First year of hourly pure methanol production

Related to the import of electricity and CO_2 , a clear correlation can be observed between both graphs. This correlation is directly linked to the operational level of the plant. When the plant has ample renewable energy supply from the solar and wind farms, its operational point reaches its maximum, leading to a higher CO_2 intake from the available stream. In these conditions, there is no need to purchase electricity from the grid, as the locally produced renewable energy is sufficient to sustain operations.

Conversely, when renewable energy production is low, the model prefers to reduce the operational level to optimize efficiency. However, since the plant must maintain minimum operational points and fulfill the required methanol demand, grid electricity imports become necessary. This results in a lower CO_2 intake, as the plant does not operate at full capacity, reflecting the direct relationship between CO_2 import and electricity availability.

Finally, the variation in the state of charge of different storage systems is directly influenced by the previous trends observed in electricity and CO_2 imports. The relationship between CO_2 imported from the CHP plant and the CO_2 stored becomes particularly intuitive. When the CO_2 flow from the stream reaches its maximum value, the state of charge of the CO_2 storage decreases. This occurs because the reactor is operating at a high point, demanding large amounts of CO_2 to sustain methanol production.

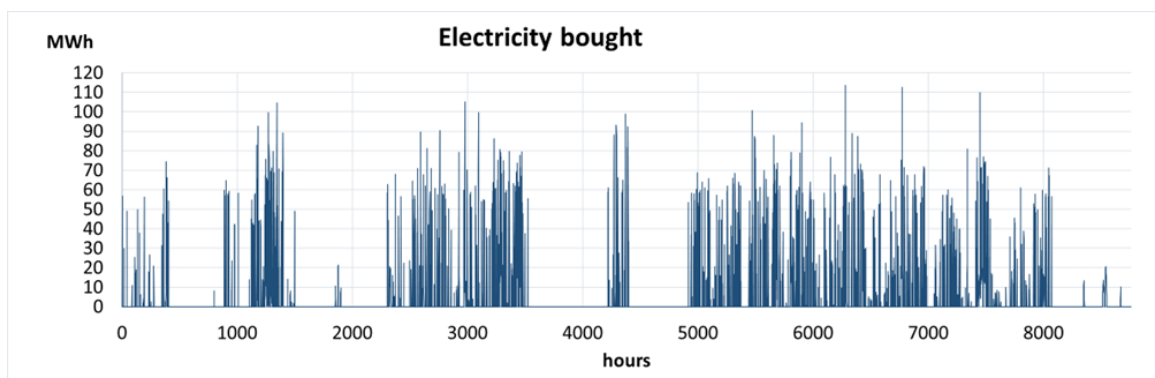


Figure 20: First year of hourly electricity imported from the grid

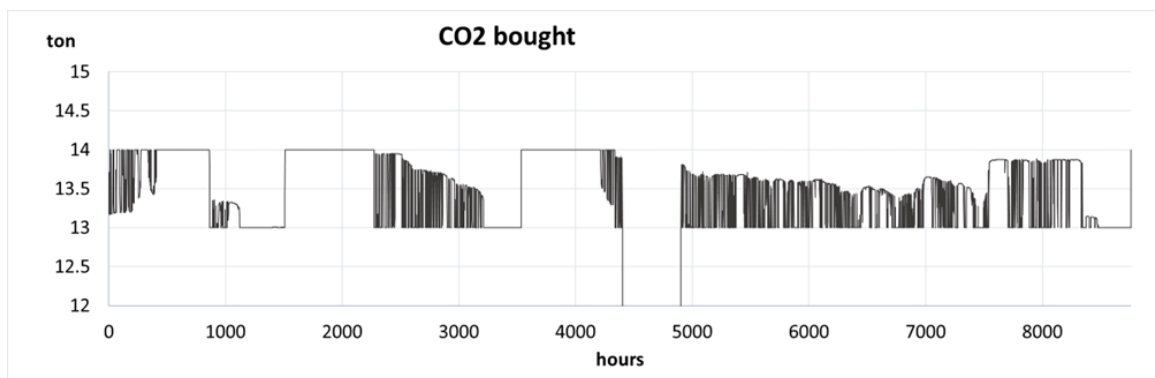


Figure 21: First year of hourly CO_2 stream from the CHP plant

Another notable observation is that the CO_2 storage and raw methanol storage behave as mirrored systems. As previously discussed, when the reactor operates at a high point, CO_2 storage is being depleted, while raw methanol storage is being filled. This reflects the natural flow of materials within the system, where increased reactor operation results in higher methanol production and higher CO_2 consumption.

Lastly, the pure methanol storage exhibits more stable variations compared to other storage systems. This is because it is primarily responsible for continuously supplying the methanol demand, while its replenishment depends on the distillation column, which operates at a steady level. The more stable operation of the distillation process ensures that pure methanol storage follows a smooth and predictable pattern, unlike the more dynamic variations observed in CO_2 and raw methanol storage.

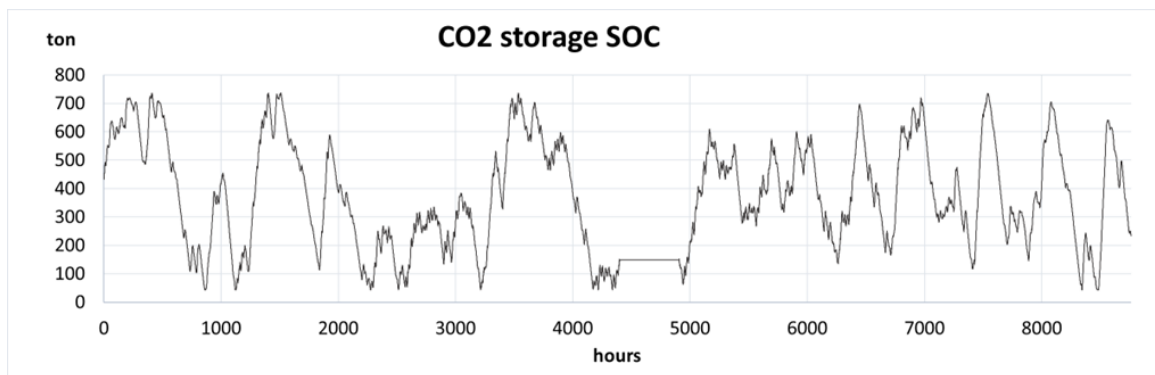


Figure 22: State of charge of the CO_2 storage

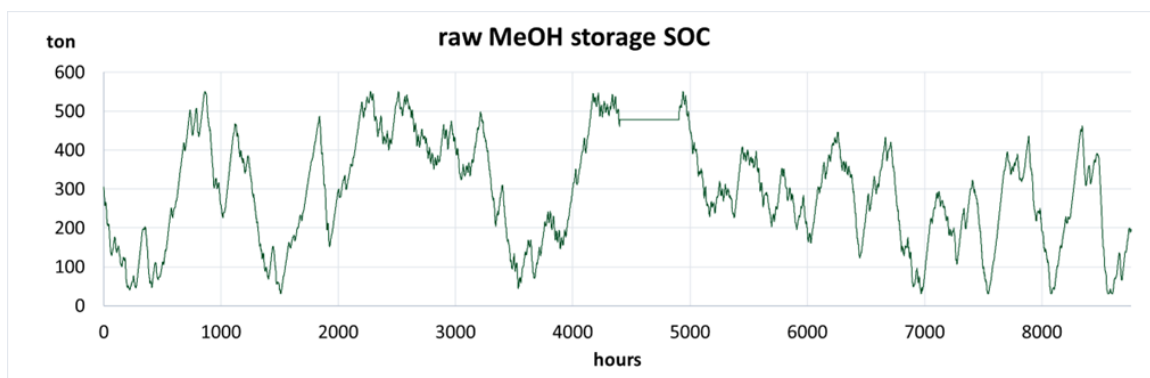


Figure 23: State of charge of the raw methanol storage

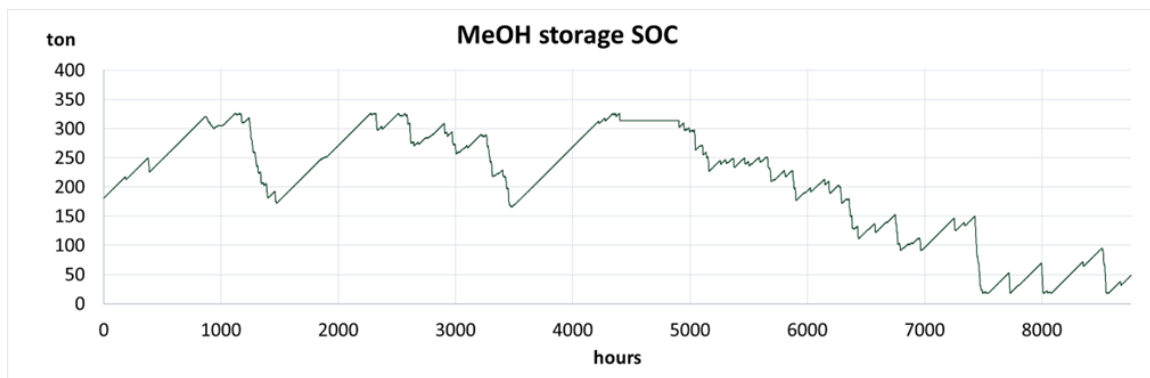


Figure 24: State of charge of the pure methanol storage

Model configuration with no grid connection

The model with no grid connection is entirely constrained by the minimum operational point, making this factor the primary driver of all results. As shown below, in order to meet the minimum operational point requirements, electricity production must be oversized. Consequently, there is an abundance of electricity during most hours, as excess energy cannot be sold back to the grid. Due to these constraints, the assets directly involved in methanol production are sized to the minimum required capacity while being forced to operate at the highest possible utilization rate. Unlike the previous configuration, where production assets may have operated at varying levels, in this case, all methanol production assets operate simultaneously to ensure the plant meets its production requirements despite the limited energy flexibility.

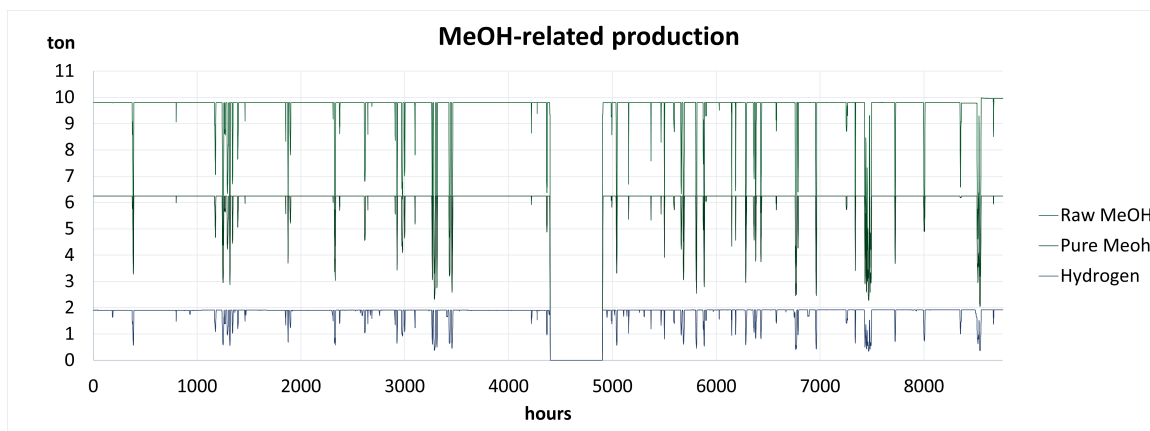


Figure 25: First year hourly production of elements directly involved with methanol

Contrary to the model configuration with grid connection, in this scenario, there is no advantage in continuously adjusting the operational point of the reactor or in varying the CO_2 stream flow from the CHP plant. Since the plant must operate within its minimum constraints and cannot rely on external electricity sources, maintaining a steady operational profile becomes the most efficient approach. As a result, the stability of methanol production assets directly impacts the feedstock purchase strategy. With fewer fluctuations in production levels, CO_2 and hydrogen consumption remain more consistent, leading to a more predictable and stable feedstock demand.

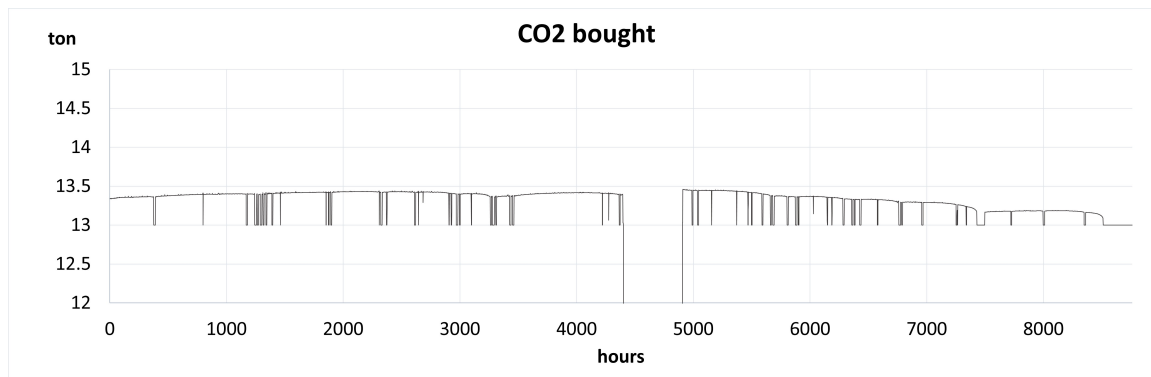


Figure 26: First year of hourly CO_2 stream from the CHP plant no grid connection

The behavior of the battery may not seem immediately intuitive, but upon closer examination, there is a clear rationale behind it. Given that the model has an excess of electricity and operates with perfect foresight, there is no need to keep the battery fully charged at all times. Instead, when additional electricity is required, the model charges the battery in the preceding hours and then discharges it as needed. As a result, the battery remains at approximately 50% charge for most of the time, optimizing its utilization without unnecessary storage.

Similar to the previous model configuration, the CO_2 purchased from the CHP plant is correlated with the battery operation. It can be observed that battery discharges coincide with periods where the CO_2 stream reaches its minimum value, indicating that methanol production is at its lowest during these moments. This relationship suggests that the battery plays a crucial role in balancing fluctuations in methanol production, ensuring that the energy supply is aligned with the availability of feedstock.

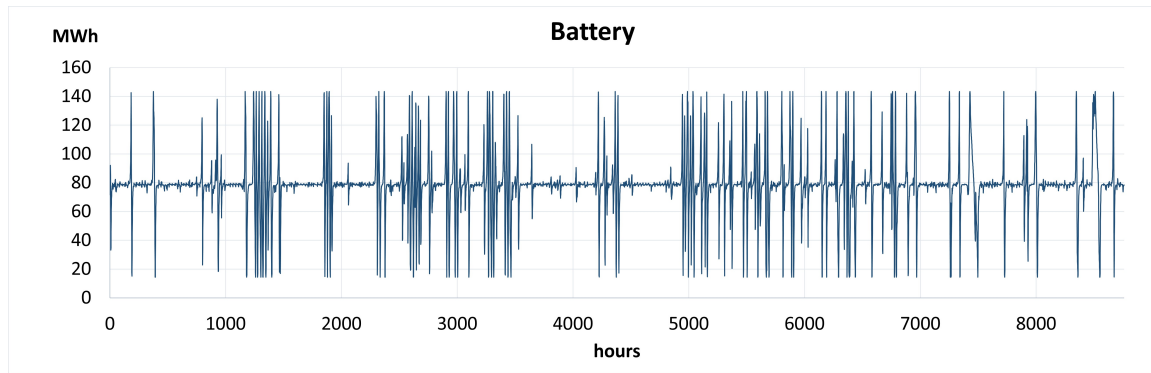


Figure 27: First year of hourly battery operation

Finally, in concordance with the previous observations, storage assets exhibit a more stable variation compared to the model configuration with grid connection. This behavior aligns with expectations, as the state of charge of the storages is directly dependent on the operation of the production assets. With no external electricity imports, the system is forced to operate within its own energy balance, leading to less fluctuation in storage levels.

It is also worth noting that this model configuration includes a significant hydrogen storage capacity, which plays a role in supporting the battery to ensure compliance with the minimum operational point constraint. The hydrogen storage serves as an additional buffer, providing flexibility to maintain steady methanol production, particularly when renewable generation is not sufficient to meet demand directly.

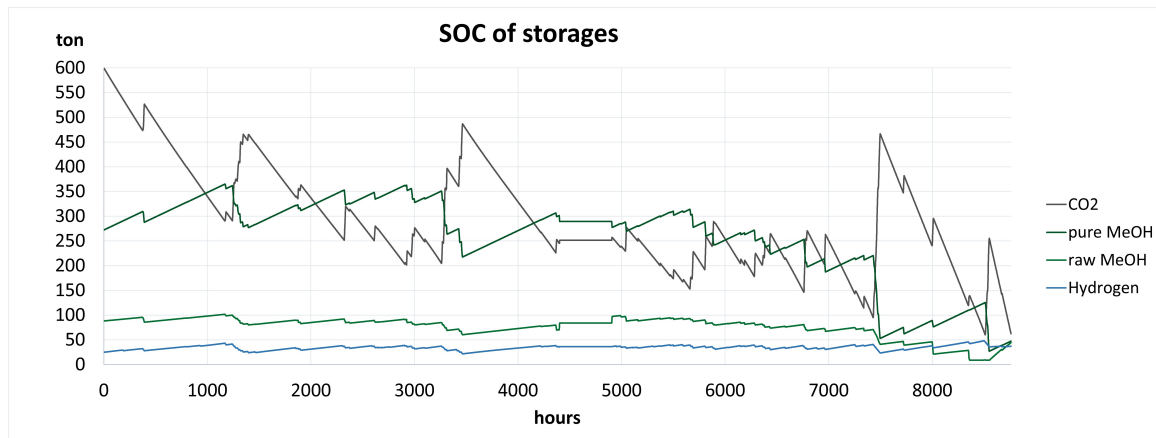


Figure 28: Combined state of charge of the storages with no grid connection

7.2 Comparison of the two model configurations

To begin with, the initial comparison focuses on the objective values, which represent the total cost across different model configurations. One of the most significant observations is that allowing electricity imports from the grid nearly doubles the total cost of the model.

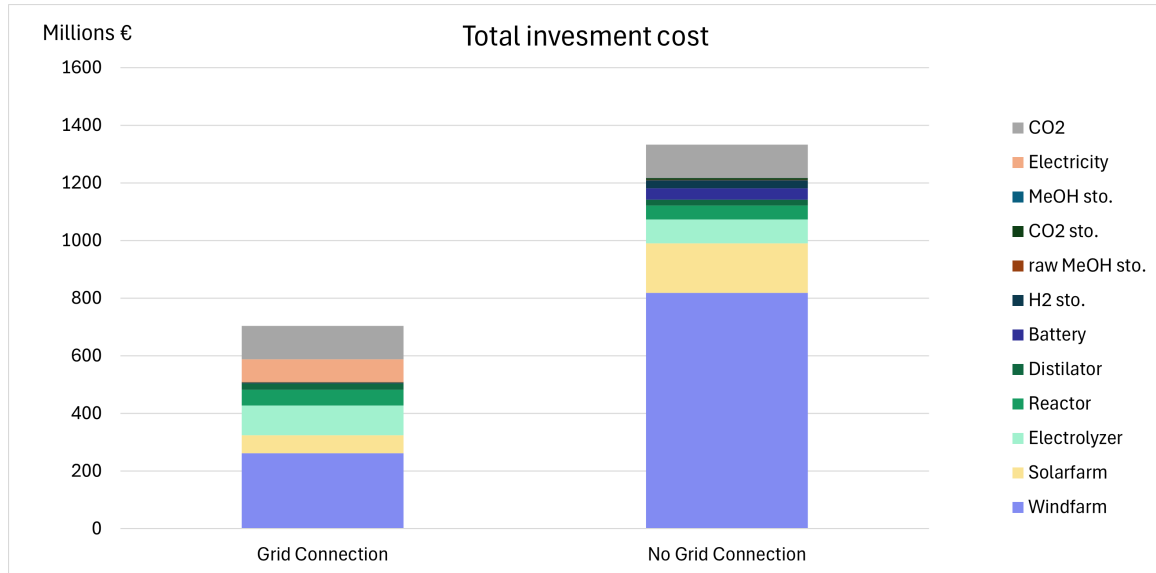


Figure 29: Comparison of costs for every model configuration

In this context, the cost difference primarily stems from the grid connection, which plays a crucial role in balancing peak demand and compensating for electricity shortages during scarcity hours. Without grid access, the reliance on energy storage solutions becomes more significant, directly impacting the total system cost. Due to the necessity of maintaining minimum operational points, the model must oversize renewable generation assets to ensure a continuous energy supply. Without grid connections, situations where neither wind nor solar produce electricity—commonly referred to as dunkelflaute—become a critical cost driver for the total investment. In such cases, the model must compensate for prolonged periods of low renewable generation, requiring larger

energy storage capacities and over-dimensioned renewable assets, significantly increasing overall costs.

Regarding variable renewable generation, it is noteworthy that solar and wind capacity remain approximately the same across both model configurations. Although the offshore wind farm has a capacity factor nearly three times higher than that of the solar farm, its cost is approximately five times greater. Despite this cost disparity, the model continues to invest in wind generation, as the methanol plant operates continuously, including nighttime hours, when solar energy is unavailable. Furthermore, the difference between solar and wind capacity becomes less pronounced because the configurations account for maintenance periods. This is due to the fact that maintenance is scheduled during summer, when daylight hours are at their highest, reducing the reliance on solar energy and making wind energy a more critical source to sustain operations. As a result, the model prioritizes wind capacity in these configurations, ensuring a stable energy supply throughout the year.

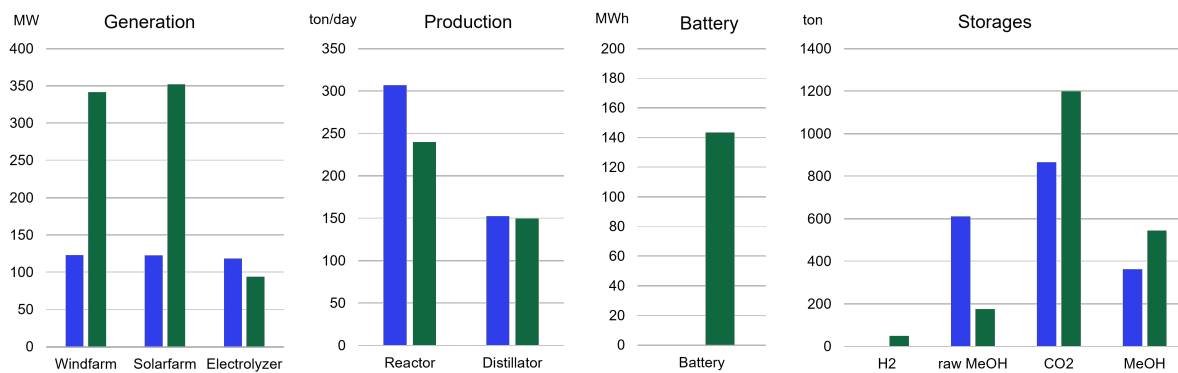


Figure 30: Comparison of capacities of the assets. Blue grid connection. Green no grid connection

The size of the assets directly involved in methanol production, such as the electrolyzer, reactor, and distillation column, is significantly larger in models that include maintenance periods. This is because these assets must compensate for downtime by increasing production within a shorter operational window. In contrast, when electricity imports from the grid are not allowed, the asset sizes tend to be smaller. This reduction occurs due to the greater investment in battery storage, which stabilizes the energy supply. As a result, production assets can operate at a more stable and optimized level, reducing the need for oversized capacity.

Storage capacities vary significantly depending on the model configuration. In general, the model tends to oversize storage assets to increase operational flexibility. However, it is important to note that the model is driven solely by the objective value, meaning it always seeks the most cost-effective configuration to achieve the minimum total cost. Examining the cost distribution in graph XXX, it is evident that the costs associated with storage assets are nearly negligible. The primary reason storage capacities are not even larger is that the model derives no additional economic benefit from further expansion. As a result, storage investment is optimized purely based on cost-efficiency, rather than any inherent preference for larger capacities.

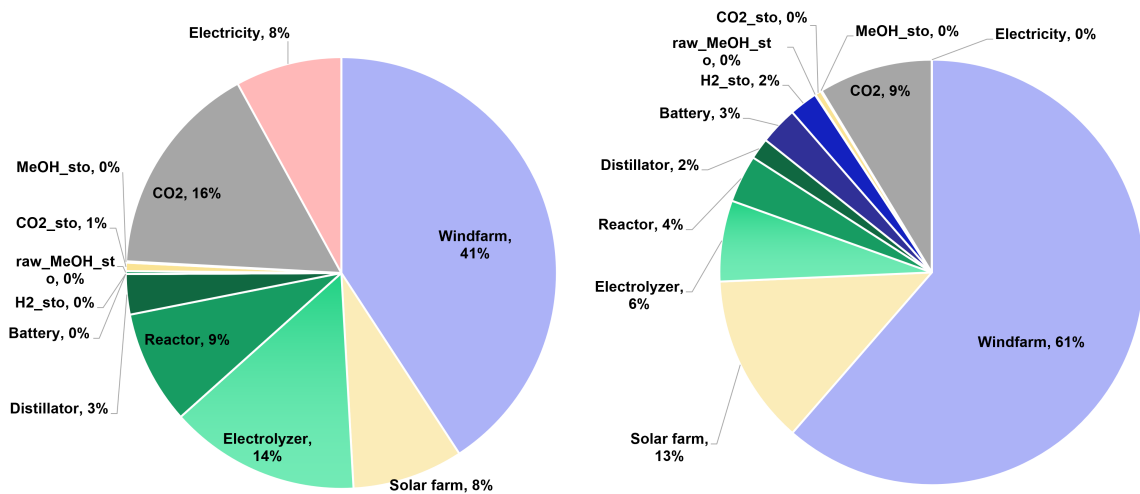


Figure 31: Cost distribution for both model configurations

Cost distribution

In order to analyze how the model allocates investments, the distribution of costs can be categorized into four main groups.

1. The first group represents the costs associated with electricity production, which account for 56% and 74% respectively of the total investment. This includes expenses related to the wind farm, solar farm, and electricity purchases from the grid. Among all categories, this group has the largest optimization potential, as electricity production offers multiple alternatives that the model can adjust to minimize costs.
2. The second group consists of CO_2 costs, which remain constant across all model configurations. The reason behind this is that CO_2 is supplied as a fixed-price stream, meaning the model cannot optimize or reduce its cost. The expense associated with CO_2 represents between 9% and 16% of the total investment, making it a significant but inflexible component of the cost structure.
3. The third group includes the assets directly involved in methanol production, specifically the electrolyzer, reactor, and distillation column. The size and cost of these assets vary depending on the model configuration, particularly in relation to electricity availability. In scenarios without grid connection, these assets tend to be smaller, as the system prioritizes energy stability over maximizing production capacity. The total cost of this category ranges between 12% and 26% of the total investment.
4. The fourth and final group consists of the five storage assets considered in the model. One of the most striking observations is that storage costs are almost negligible compared to the overall investment. As a result, the model tends to oversize storage assets without significant financial implications. The total cost of storage systems can reach up to 5% of the total investment, depending on the specific model configuration.

Distribution of electricity production

To start with, when analyzing energy production, it is evident that, given the same installed capacity for wind and solar, and considering that wind has a capacity factor approximately three times higher than solar, the relationship between their total electricity generation follows a similar pattern. However, a key observation is the significance of electricity purchased from the grid in the overall energy mix.

A particularly notable comparison is between solar-generated electricity and grid-purchased electricity. The total electricity produced by solar farms is around four to five times higher than the

electricity imported from the grid. However, when comparing costs, it becomes clear that the total investment in solar panels is similar than the total cost of electricity purchased from the grid.

This finding emphasizes the economic impact of grid reliance, as continuously purchasing electricity can result in higher long-term expenses compared to an upfront investment in renewable assets. The following section presents a breakdown of electricity costs from different sources, further highlighting the financial trade-offs between on-site generation and grid dependency.

Source	LCOE
Wind	483 €/MWh
Solar	332 €/MWh
Grid	1440 €/MWh

Table 13: Levelized Cost Of Electricity

This leads to two main conclusions:

- Electricity produced by the solar panels can be up to four times lower than the one proceeding from the grid.
- The cost of electricity availability can be extremely high when it is required, and therefore, the model cannot cut down in expenses related to this point.

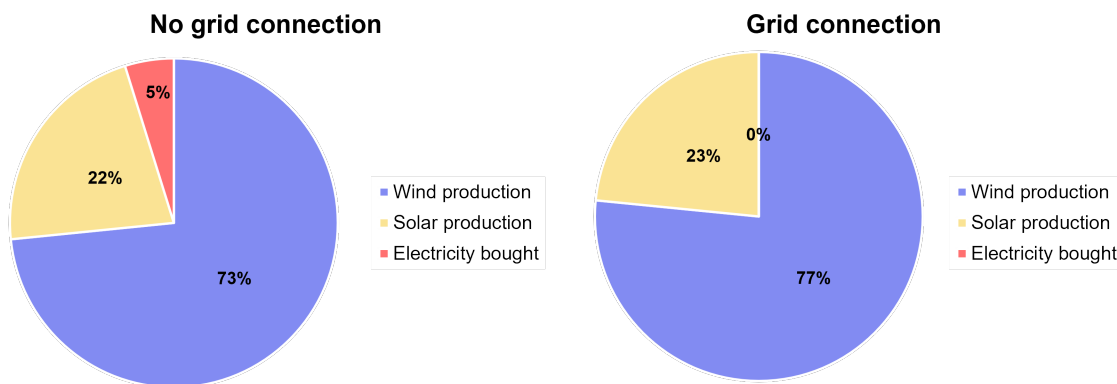


Figure 32: Source of electricity production across model configurations

Distribution of electricity consumption

Regarding energy consumption, two key aspects should be highlighted:

- First and foremost, the vast majority of electricity is consumed by the electrolyzer. Other demands, such as heating and desalination, become negligible in comparison to the energy required for hydrogen production. Given this, in a large-scale model or further analyses, these smaller energy demands could be omitted without significantly affecting the overall results.
- The second important point is the amount of electricity that must be curtailed, as selling electricity back to the grid is not permitted in this model. It can be observed that in configurations where no grid connection is considered, the curtailed electricity can reach up to two-thirds of the total production. Additionally, grid imports also influence electricity curtailment. Since the methanol plant must meet a constant demand every hour, electricity production assets must be oversized to ensure reliability. As a result, during periods of maximum production, an extremely amount of excess electricity is wasted.

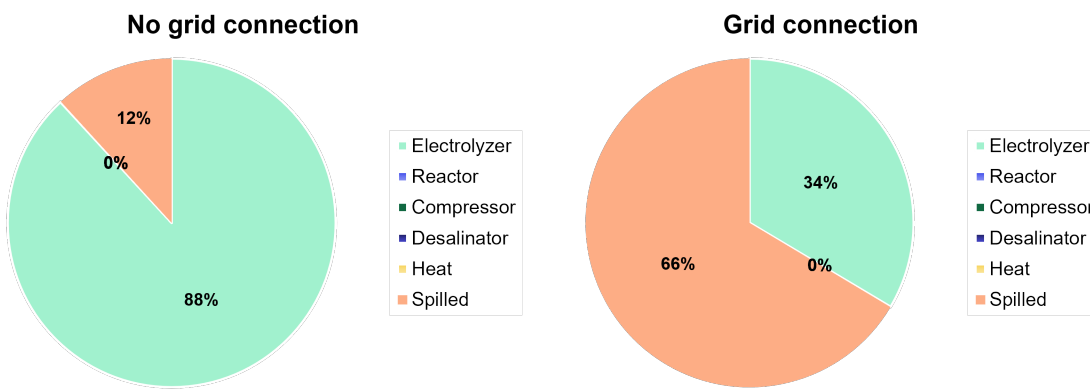


Figure 33: Electricity consumption across model configurations

7.3 Levelized Cost of Methanol (LCOM)

LCOM represents the total cost of producing methanol over the lifetime of a plant. It is calculated using the following formula:

$$LCOM = \frac{\sum \text{Total Costs(CAPEX + OPEX + Feedstock + Energy)}}{\sum \text{Total Methanol Produced Over Lifetime}} \quad (7.1)$$

Since four different model configurations have been implemented, four different LCOM values have been obtained. It is important to note that the total methanol produced over time also needs to be annualized.

	Grid connection	No Grid connection
LCOM (€/ton)	1387	2558

Table 14: Levelized Cost of Methanol (LCOM) for Different Model Configurations

Validation of results

After accounting the LCOM, next step is to compare results with external sources and analyze if they are realistic and feasible. Hence, validation has been based on two different sources. These surces are IRENA (International Renewable Energy Agency)[34] and the Royal Society of Chemistry[35]. Thus, the LCOM that these sources apport are reflected in the following table:

	IRENA	RS of Chemistry
LCOM (€/ton)	760 - 1540*	600 – 680

Table 15: Levelized Cost of Methanol (LCOM) based on literature

*Note: currency conversion has been applied by 0.95€ corresponding to 1 USD.

It is worth mentioning that, according to IRENA, the current production cost of e-methanol is estimated to be in the range of USD 800-1,600 per ton, assuming that CO_2 is sourced from BECCS at a cost of 10-50 USD per ton.

For the Royal Society of Chemistry, the adopted assumption has been based on a Levelized Cost of Electricity (LCOE) in the range of 94–107 € per MWh.

Based on these results, the model configuration aligns with IRENA's estimated cost range, suggesting that the assumptions made for CO_2 sourcing and electricity costs are consistent with global projections. However, the model does not fall within the cost range proposed by the Royal

Society of Chemistry, likely due to differences in assumed electricity prices or additional cost factors considered in the study. Additionally, the configuration without grid connection significantly exceeds these cost estimates, primarily due to the higher capital expenditure required for oversized renewable generation and storage assets to ensure continuous operation without external electricity imports.

7.4 Results related to decomposition techniques

To begin with, the implementation of the full algorithm, incorporating both decomposition techniques, was unsuccessful. To address this issue, an analysis was conducted, as the real issue would have been failing to identify the root cause of the failure. The immediate reason for the error was that the CPU ran out of memory, causing the process to stop. This occurred because the Master problem in the Dantzig-Wolfe algorithm accumulated too many constraints without making sufficient progress. Upon deeper analysis, it was determined that the issue stemmed from the state of charge (SOC) constraint of the storage systems 6.1. The equality constraint enforced identical SOC values in both subproblems at the points where they were linked in the master problem. However, due to precision limitations, the SOC values never matched exactly, preventing the model from converging. Following this realization, it was decided to proceed with an alternative decomposition approach. While it was demonstrated that Dantzig-Wolfe was not effective, this did not rule out the possibility that Benders decomposition could still prove to be a viable solution.

The results for Benders decomposition were different from another nature than those of Dantzig-Wolfe. The main issue with this approach was the long running times. Since the subproblem could not be further divided into smaller parts, the algorithm ended up with a small Master problem — which is desired — but a very large subproblem. As a result, solving the subproblem took longer than expected. It is also important to note that Benders subproblems must be solved to optimality. If they were not, the solutions they provide would not help improve the Master problem's solution, making the whole process ineffective.

When solving the problem on the same laptop used for the original implementation, the simulation continued running for more than four days without reaching a final solution. Although the solution was improving with each iteration, the progress was not fast enough. As a result, a larger computing system was required. Utilizing the university's supercomputer, the problem was running within the 24-hour time limit imposed by the system. It is important to note that the algorithm allows for stopping and resuming from the last iteration if needed. However, this was not considered necessary in this case. Instead, to demonstrate the full implementation of the model, a one-year simulation was conducted, having scaled electricity and CO_2 prices over the running period. The results provide insights into the evolution of the assets, as well as the upper and lower bounds of the solution. As a note, the asset sizes are represented in per-unit values, meaning that the values shown indicate the ratio between the actual asset size and its maximum possible capacity.

In the first two graphs, the results from the initial XX iterations are presented. It can be observed that the solution continuously improves after each iteration, as expected. One key observation is that, at the beginning, the model prioritizes maximizing the size of the storage assets without initially considering the need to invest in assets directly involved in methanol production. This behavior suggests that the algorithm first seeks to increase storage capacity before optimizing the overall system investment strategy.



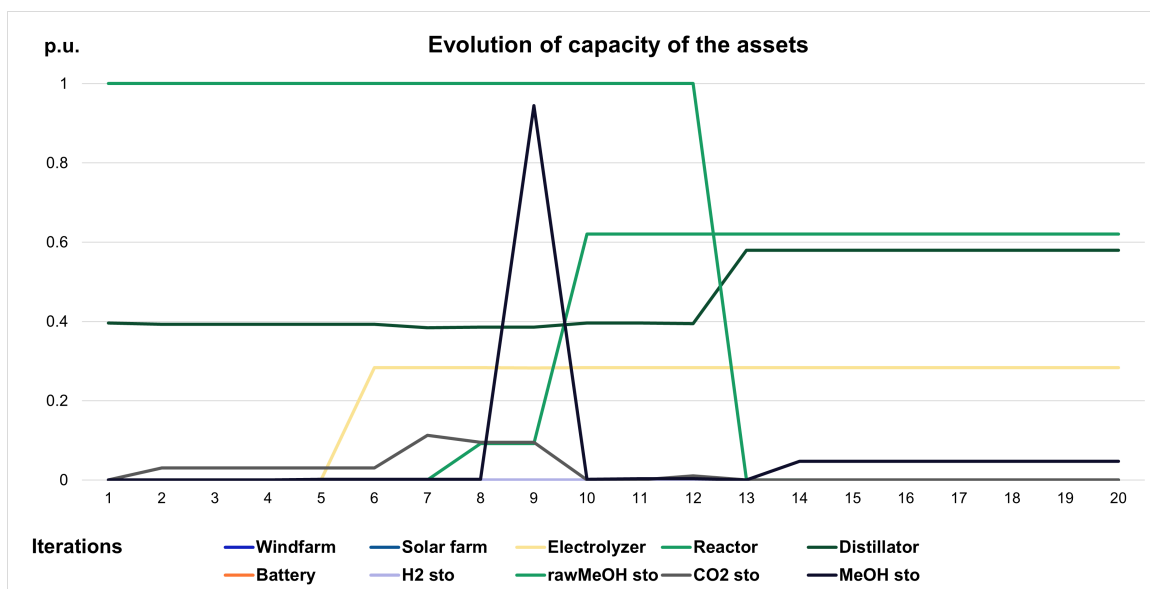


Figure 34: Evolution of the asset sizes for the whole model

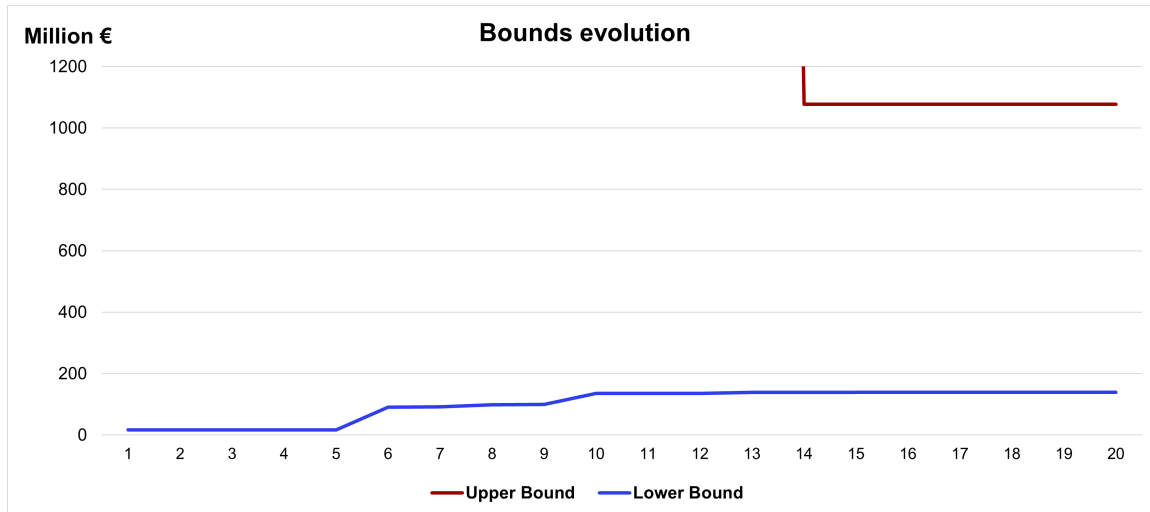


Figure 35: Lower bound evolution for the whole model

During the execution of the algorithm, the model initially prioritizes upgrading storage assets. This is because, at the start, the model takes a myopic approach, where investing in storage provides a quick solution to meet demand, given that storage assets begin at 50% capacity. After several iterations, the model recognizes the need to invest in assets directly related to methanol production since it is also required to maintain storage at 50% capacity at the end of the simulation period. Finally, the model shifts its focus toward investing in electricity generation capacity. Initially, it relies entirely on electricity from the grid, but over time, it determines that this is not the most effective strategy and allocates resources to energy assets to improve efficiency and reduce dependency on external electricity sources.

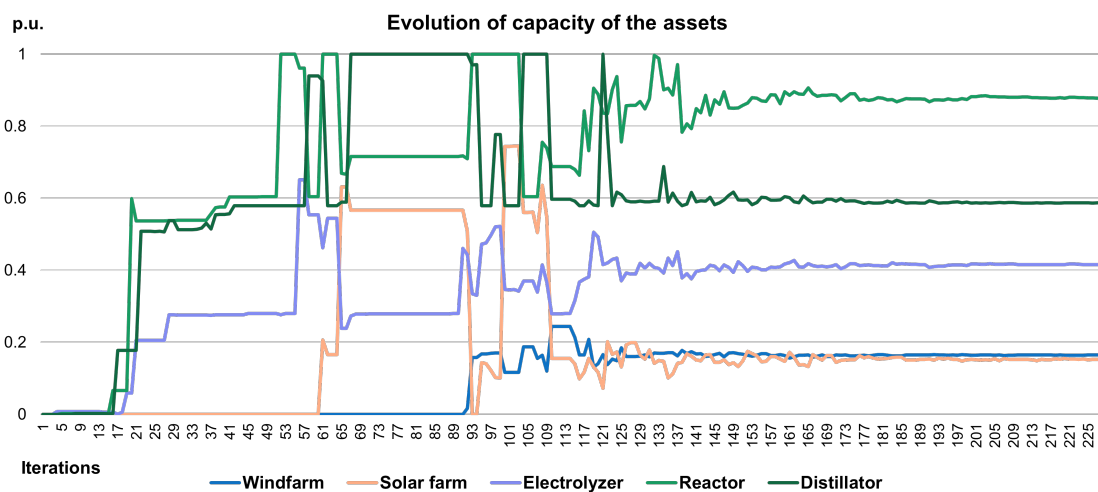


Figure 36: Evolution of the asset sizes for the one-year model

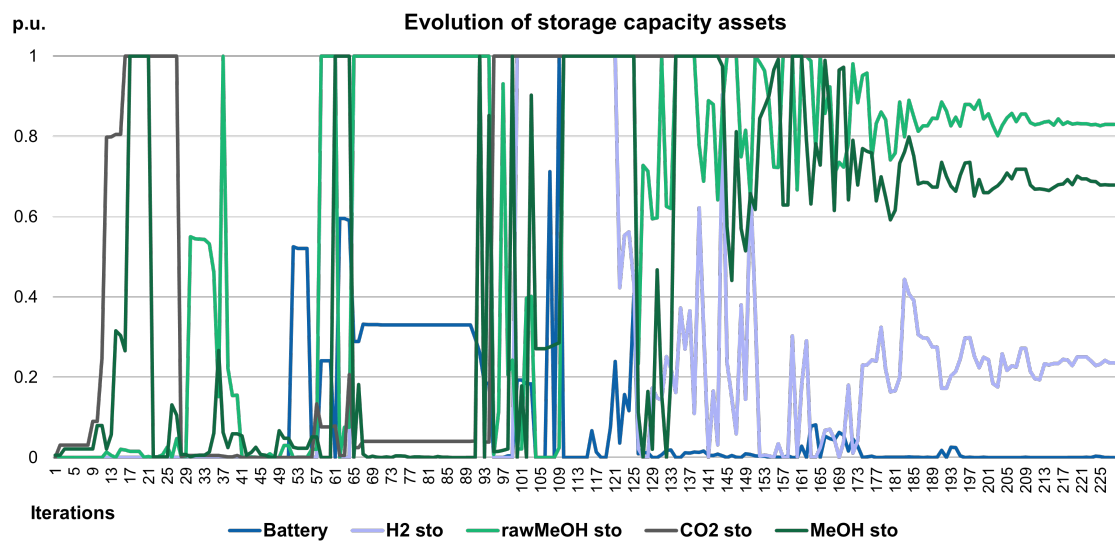


Figure 37: Evolution of the storage asset sizes for the one-year model

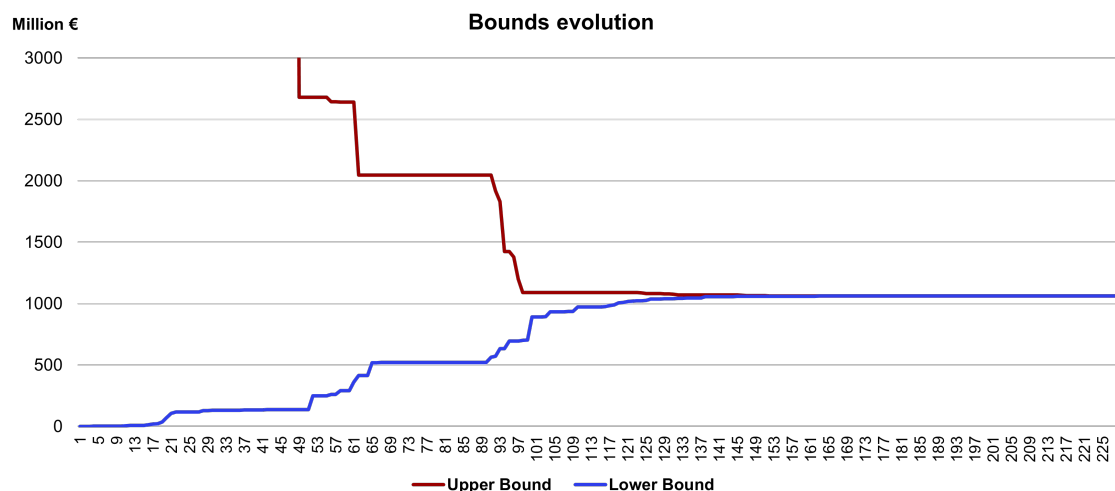


Figure 38: Bounds evolution for the one-year model

In the bounds evolution graph, it is intuitive to see how the lower bound — defined by the master problem — starts at zero. This occurs because, in the first iteration, the master problem is unconstrained, leading to a minimum objective value where all asset capacities are set to zero. With each iteration, as constraints are added and asset capacities are adjusted, the lower bound increases. On the other hand, the upper bound is determined by the subproblem, which is a maximization problem. During the first few iterations, the subproblem remains infeasible, preventing the definition of an upper bound. However, after a few iterations, the assets grow large enough to make the subproblem feasible, allowing it to provide a valid upper bound.

Lastly, an interesting observation is that forcing a minimum asset size does not provide any benefit. Before solving the problem, an initial estimation suggested that a minimum capacity for methanol production assets — such as the electrolyzer, reactor, and distillation column — would be necessary. However, implementing this constraint did not improve the solution. The model still followed the same investment pattern, first prioritizing storage assets before expanding production-related capacities. More importantly, the number of iterations required to reach optimality remained nearly the same, indicating that adding a minimum capacity constraint did not significantly impact the convergence behavior.

7.5 Computational values

The original model is composed by 16,829,961 rows, 9,466,858 columns and 42,995,302 non-zeros, where the rows represent constraints, the columns correspond to variables, and the non-zero values represent the elements within the entire model. The solution process took approximately between 1.5 to 2 hours.

The model was solved using a laptop with the following properties: CPU model: Intel(R) Core(TM) i7-8550U CPU @ 1.80GHz, instruction set [SSE2|AVX|AVX2] Thread count: 4 physical cores, 8 logical processors, using up to 8 threads.

The Benders decomposition model run for 24 hours in DTU's supercomputer with the following properties: CPU model: Intel(R) Xeon(R) CPU E5-2660 v3 @ 2.60GHz, instruction set [SSE2|AVX|AVX2] Thread count: 20 physical cores, 20 logical processors, using up to 20 threads.



8 Sensitivity analysis

In order to assess the relevance of different parameters in the model, sensitivity analyses must be performed. These analyses focus on factors that exhibit high variability or uncertainty while also being critical to the model's outcomes.

For this study, the impact of grid connection and electricity prices has been analyzed, as both factors directly influence the overall system cost and operational feasibility. The grid connection determines whether the plant can import electricity, affecting renewable asset sizing and storage requirements. Meanwhile, electricity prices are subject to market fluctuations and policy changes, making them a key driver of production costs.

By conducting sensitivity analyses on these parameters, the study aims to quantify their impact on the model's economic performance and identify potential cost optimization strategies.

8.1 Grid connection

As demonstrated above, the possibility of importing electricity from the grid is a key driver of the model's economic performance. Among the two analyzed configurations, it has been shown that not establishing a constant flow of electricity is compensated by oversizing renewable generation assets. This trade-off highlights how the absence of grid access leads to higher capital expenditures in local generation and storage.

However, what has not yet been analyzed is the maximum grid import capacity required to stabilize costs without significantly increasing the total investment. To assess this, grid connection has been progressively constrained using various limiting parameters, allowing for an evaluation of its implications and correlation with the overall investment cost of the model. This analysis helps determine an optimal grid import capacity, balancing cost efficiency and system reliability. The grid variation has been assessed in increments of 10 MW, allowing for a detailed evaluation of its impact on total system costs and operational efficiency.

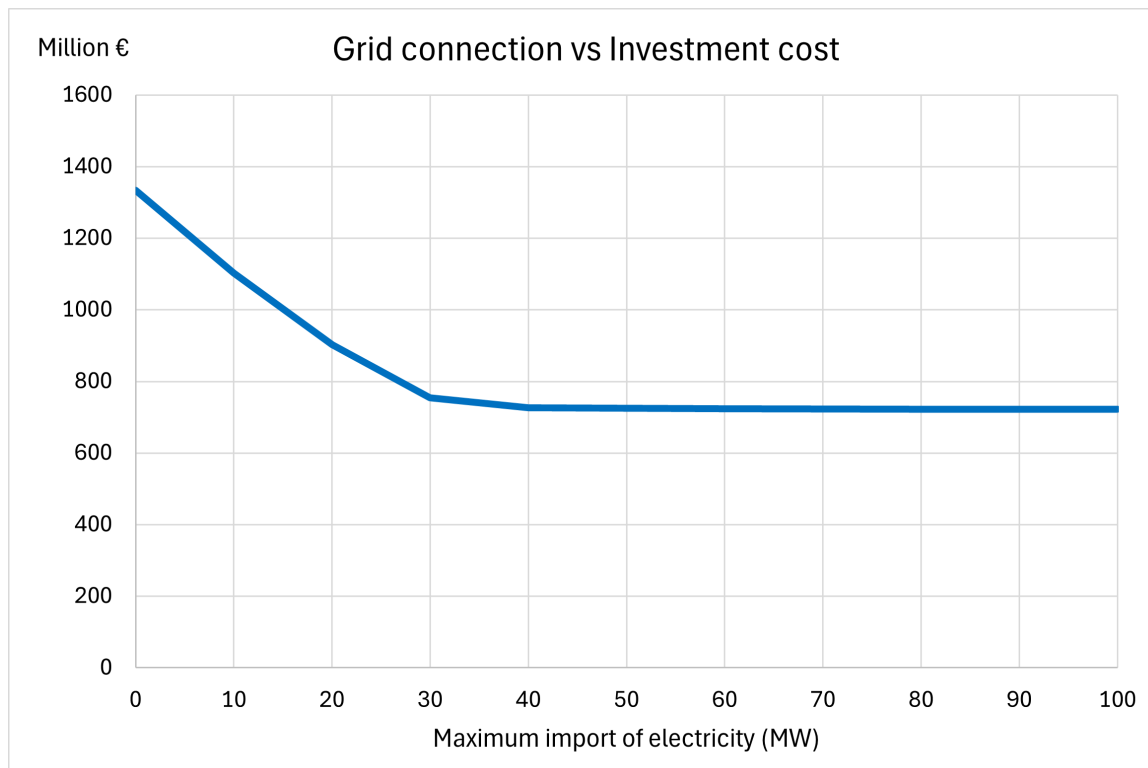


Figure 39: Comparison between maximum electricity import from the grid and total investment cost

From the results observed in the graph above, it can be noted that the curve remains flat for grid import limits above 30 MW. This indicates that strengthening the grid connection beyond this threshold does not provide significant additional benefits, as instances where electricity imports exceed this value are rare. In other words, further increasing grid capacity would not substantially reduce total investment costs, as the model does not frequently require imports beyond this level. Additionally, a comparison can be made between the maximum electricity imported from the grid and the size of the electrolyzer, which represents the maximum electricity demand of the system. The electrolyzer capacity is approximately 120 MW, with small variations depending on the grid limit. Based on this, it can be inferred that a reasonable assumption for grid connection capacity should be at least one-fourth of the electrolyzer capacity. Furthermore, it is important to recall that the minimum operational point of the electrolyzer is 15% of its total capacity, which corresponds to an hourly electricity consumption of approximately 18 MW. This reinforces the idea that a grid connection limit significantly below one-third of the electrolyzer capacity could introduce operational constraints, while higher values may offer limited economic advantages.

8.2 Electricity prices

To assess the impact of average electricity prices on the model, a sensitivity analysis was conducted by modifying the input electricity price data using a scaling factor. The analysis focused on the energy generation sector, as this was the most affected area. The results were evaluated based on changes in overall investment cost, wind capacity, and solar capacity, with comparisons made against the base case (no price variation).

The results indicate that the impact of electricity price variation is asymmetrical. A 25% reduction in electricity prices caused a greater variation in investment decisions compared to a 25% increase. The reason behind this is that lower electricity prices encouraged the model to reduce investments in renewable generation assets, reallocating capital toward purchasing more electricity from the grid. Conversely, an increase in electricity prices had a limited impact on total investment, as the model maintained a similar asset allocation strategy.

In the most extreme scenario—where electricity prices were doubled—the total investment cost increased by only 4%, suggesting that electricity price levels do not strongly influence the model's overall cost structure. Instead, the availability of grid electricity plays a more crucial role in determining investment decisions.

Overall, the findings show that generation asset sizes change more significantly when electricity prices decrease by 25% than when they increase by 100%, implying that the model is robust to electricity price volatility.

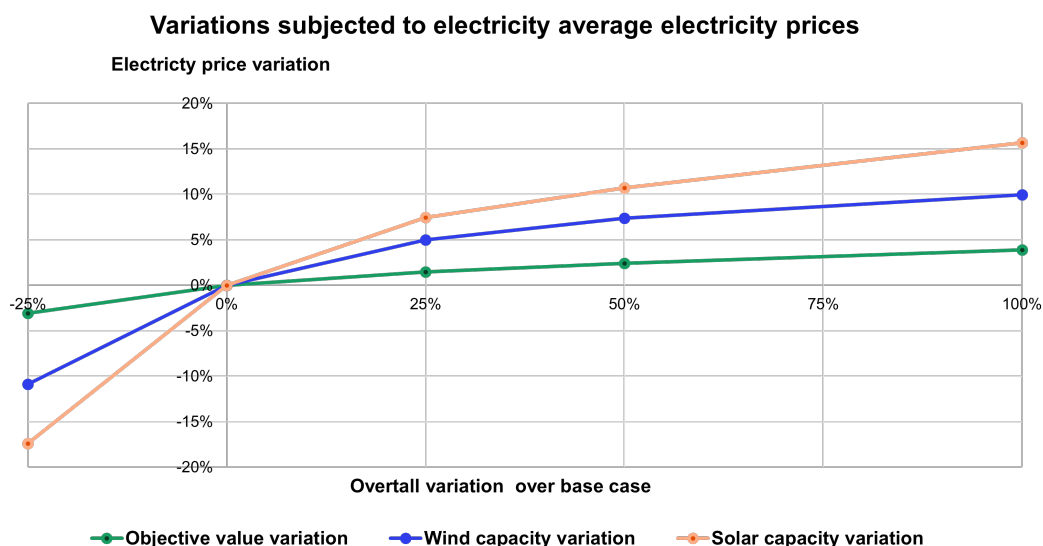


Figure 40: Comparison between electricity prices variation with base case model

9 Limitations and possible improvements

To critically evaluate the assumptions made in the model, an analysis of its limitations and possible improvements has been conducted. The most relevant points are outlined below:

1. Perfect Forecast Over 30 Years

The model assumes perfect knowledge of future conditions, as input data remains unchanged over time.

Improvement: Introduce stochastic optimization and scenario-based projections to account for uncertainty and long-term variability.

2. No Correlation in Electricity Prices

The model treats electricity prices as independent variables, unrelated to wind and solar generation.

Improvement: Implement time series analysis to establish correlations between electricity prices and renewable generation for a more realistic approach.

3. Uncertainty in Offshore Wind Costs

Due to market fluctuations and evolving technology, offshore wind costs can vary significantly.

Improvement: Conduct a detailed cost analysis incorporating current market trends and project-specific conditions.

4. Solar Capacity Does Not Consider Land Cost and Space Availability

Land requirements for solar installations are not factored into the model, potentially underestimating real-world constraints.

Improvement: Include land cost and spatial availability constraints when modeling solar capacity.

5. CO₂ Cost Variability

CO₂ costs lack a well-defined market, leading to large uncertainties depending on the source.

Improvement: Study existing projects to obtain more accurate cost estimates for CO₂ as a feedstock.

6. Oversized Storage Capacity

Due to its relatively low cost compared to the overall system, storage tends to be oversized in the model.

Improvement: Introduce space availability constraints to prevent unrealistic storage expansion.

7. Fixed and Uncertain Demand

The model assumes a fixed demand, despite the uncertainty in the future methanol market due to political and economic factors.

Improvement: Implement scenario-based demand forecasting to account for policy changes and market development.

8. Simplifications in Asset Operation

The model does not consider efficiency variations across different operational points, leading to simplified performance assumptions.

Improvement: Increase model complexity by incorporating operational efficiency curves, if computationally feasible.

9. Simplified Asset Investment Costs

Investment costs are modeled as solely dependent on asset size, without considering feasibility constraints or real-world construction costs.

Improvement: Perform detailed feasibility studies to refine asset investment cost assumptions.



10 Conclusion

The study successfully developed an optimization model to determine the optimal sizing of assets for a methanol production plant. The largest share of the investment (56% to 74%) was allocated to electricity production, with wind and solar capacities remaining similar across model configurations.

The application of Benders and Dantzig-Wolfe decomposition techniques was explored. While Dantzig-Wolfe decomposition faced infeasibility issues due to State of Charge (SOC) constraints in storages, Benders decomposition proved to be a feasible approach but required high computational effort. Furthermore, Benders decomposition could become more advantageous when stochastic optimization is introduced, as the problem would naturally decompose into multiple subproblems, enhancing computational efficiency and scalability.

In the grid-connected model configuration, approximately 12% of the produced electricity is curtailed, whereas in the off-grid configuration, nearly 66% of the generated electricity needed to be curtailed. This significant difference highlights the inefficiency of excess renewable energy production in an off-grid scenario, where the inability to sell surplus electricity or optimize its usage leads to substantial energy wastage.

A key finding was that grid electricity availability significantly affects cost minimization. In scenarios where grid imports were restricted, the model had to oversize renewable generation assets, leading to higher capital investments. A sensitivity analysis revealed that a minimum grid connection of 30 MW is recommended, as further increasing the grid import capacity beyond this value did not provide additional benefits.

It was revealed through a sensitivity analysis that electricity price variations have a limited impact on total investment costs, with grid availability playing a more crucial role. A 25% price reduction led to greater shifts in investment than a 100% increase, as lower prices encouraged grid reliance over renewable investments. Even when electricity prices doubled, total investment costs rose by only 4%, suggesting that the model is robust to price volatility, with grid access being a stronger determinant of cost efficiency.

When determining optimal asset sizing, the model avoided investments in hydrogen storage tanks and Na-Cl batteries due to their high cost relative to their benefits. Additionally, auxiliary equipment such as the desalinator, heater, and compressor had minimal influence on the model's performance. To reduce computational complexity, these components could be excluded from future model implementations.

Finally, the Levelized Cost of Methanol (LCOM) calculated by the model aligns with external sources such as IRENA. The results indicate that LCOM depends strongly on grid connection availability, with values of 1387 €/ton for grid-connected configurations and 2558 €/ton for off-grid configurations. These findings reinforce the feasibility of large-scale methanol production as a viable pathway for decarbonization, adding hope that sustainable fuels can play a key role in the green transition and a cleaner future for the maritime sector.



References

- [1] United Nations Framework Convention on Climate Change. “Key Aspects of the Paris Agreement”. In: (). URL: <https://unfccc.int/most-requested/key-aspects-of-the-paris-agreement>.
- [2] International Maritime Organization. *Fourth IMO GHG study 2020*. International Maritime Organization, 2020.
- [3] International Chamber of Shipping. *Reducing CO₂ emissions to zero: the ‘Paris Agreement for Shipping’*. International Chamber of Shipping, 2018.
- [4] International Maritime Organization. *Resolution MEPC.304(72)*. International Maritime Organization, 2018.
- [5] A.P. Moller - Maersk. “A.P. Moller - Maersk accelerates net-zero emission targets to 2040 and sets milestone 2030 targets”. In: (2022). URL: [https://www.maersk.com/news/articles/2022/01/12/apmm-accelerates-netzero-emission-targets-to-2040-and-sets-milestone-2030-targets](https://www.maersk.com/news/articles/2022/01/12/apmm-accelerates-net-zero-emission-targets-to-2040-and-sets-milestone-2030-targets).
- [6] Reuters. “Container shippers hedging green transition with dual-fuel vessel orders”. In: (2023). URL: <https://www.reuters.com/sustainability/climate-energy/container-shippers-hedging-green-transition-with-dual-fuel-vessel-orders-2024-11-21/>.
- [7] Nicolas Campion et al. “Techno-economic assessment of green ammonia production with different wind and solar potentials”. en. In: *Renewable and Sustainable Energy Reviews* 173 (Mar. 2023), p. 113057. ISSN: 13640321. DOI: 10.1016/j.rser.2022.113057. URL: <https://linkinghub.elsevier.com/retrieve/pii/S1364032122009388> (visited on 02/23/2025).
- [8] Simone Mucci, Alexander Mitsos, and Dominik Bongartz. “Cost-optimal Power-to-Methanol: Flexible operation or intermediate storage?” en. In: *Journal of Energy Storage* 72 (Nov. 2023), p. 108614. ISSN: 2352152X. DOI: 10.1016/j.est.2023.108614. URL: <https://linkinghub.elsevier.com/retrieve/pii/S2352152X2302011X> (visited on 02/21/2025).
- [9] Wärtsilä. “Methanol Engines: A Sustainable Fuel Solution for Maritime Applications”. In: (2023). URL: <https://www.wartsila.com/marine/products/engines-and-generating-sets/methanol-engines>.
- [10] Georgia Voniati et al. “Ammonia as a Marine Fuel towards Decarbonization: Emission Control Challenges”. en. In: *Sustainability* 15.21 (Nov. 2023), p. 15565. ISSN: 2071-1050. DOI: 10.3390/su152115565. URL: <https://www.mdpi.com/2071-1050/15/21/15565> (visited on 02/23/2025).
- [11] K. Machaj et al. “Ammonia as a potential marine fuel: A review”. en. In: *Energy Strategy Reviews* 44 (Nov. 2022), p. 100926. ISSN: 2211467X. DOI: 10.1016/j.esr.2022.100926. URL: <https://linkinghub.elsevier.com/retrieve/pii/S2211467X22001201> (visited on 02/23/2025).
- [12] ACS Publications. “Carbon Capture for Methanol Production: Enabling a Circular Carbon Economy”. In: *Energy & Fuels* (2022). URL: <https://pubs.acs.org/doi/10.1021/acs.energyfuels.2c00620>.
- [13] The Guardian. “Denmark Showing the World What is Possible with North Sea Green Power Plant”. In: (2025). URL: <https://www.theguardian.com/delivering-the-energy-transition/2025/feb/04/denmark-showing-world-possible-north-sea-green-power-plant-europe>.
- [14] Statista. “Forecasted Supply of Methanol as Fuel in the Shipping Industry”. In: (2024). URL: <https://www.statista.com/statistics/1367302/forecasted-supply-methanol-fuel-shipping-industry/>.

- [15] INRIA. “Efficient Optimization of Large-Scale Systems Using Decomposition Methods”. In: (2022). URL: <https://inria.hal.science/hal-03521369v1/document>.
- [16] Rodolphe Griset et al. “Combining Dantzig-Wolfe and Benders decompositions to solve a large-scale nuclear outage planning problem”. en. In: *European Journal of Operational Research* 298.3 (May 2022), pp. 1067–1083. ISSN: 03772217. DOI: 10.1016/j.ejor.2021.07.018. URL: <https://linkinghub.elsevier.com/retrieve/pii/S0377221721006135> (visited on 02/23/2025).
- [17] A. Zakaria et al. “Uncertainty models for stochastic optimization in renewable energy applications”. en. In: *Renewable Energy* 145 (Jan. 2020), pp. 1543–1571. ISSN: 09601481. DOI: 10.1016/j.renene.2019.07.081. URL: <https://linkinghub.elsevier.com/retrieve/pii/S0960148119311012> (visited on 02/23/2025).
- [18] Antonio Frangioni and Bernard Gendron. “A stabilized structured Dantzig–Wolfe decomposition method”. en. In: *Mathematical Programming* 140.1 (Aug. 2013), pp. 45–76. ISSN: 0025-5610, 1436-4646. DOI: 10.1007/s10107-012-0626-8. URL: <http://link.springer.com/10.1007/s10107-012-0626-8> (visited on 02/23/2025).
- [19] Gregor Erbach and Sara Svensson. *EU rules for renewable hydrogen*. Apr. 2023. URL: [https://www.europarl.europa.eu/RegData/etudes/BRIE/2023/747085/EPRS_BRI\(2023\)747085_EN.pdf](https://www.europarl.europa.eu/RegData/etudes/BRIE/2023/747085/EPRS_BRI(2023)747085_EN.pdf).
- [20] S&P Global. “Ørsted Scraps Swedish FlagshipONE E-Methanol Project”. In: (2024). URL: <https://www.spglobal.com/commodity-insights/en/news-research/latest-news/energy-transition/081524-orsted-scaps-swedish-flagshipone-e-methanol-project-under-development>.
- [21] Industry Decarbonization. “The Canceled Swedish E-Methanol Factory May Rise from the Ashes”. In: (2024). URL: <https://industrydecarbonization.com/news/the-canceled-swedish-e-methanol-factory-may-rise-from-the-ashes.html>.
- [22] Ørsted. “Ørsted Partners with Liquid Wind and Expands Presence in Green Fuels”. In: (2022). URL: <https://orsted.com/en/media/news/2022/01/orsted-partners-with-liquid-wind-and-expands-presence-in-green-fuels-with>.
- [23] Jingbo Wang et al. “Water electrolyzer operation scheduling for green hydrogen production: A review”. en. In: *Renewable and Sustainable Energy Reviews* 203 (Oct. 2024), p. 114779. ISSN: 13640321. DOI: 10.1016/j.rser.2024.114779. URL: <https://linkinghub.elsevier.com/retrieve/pii/S1364032124005057> (visited on 02/21/2025).
- [24] Megavind. “LCOE Model Guidelines and Documentation”. In: (2020). URL: <https://hvopen.brage.unit.no/hvopen-xmlui/bitstream/handle/11250/2679327/Megavind%20LCOE%20Model%20Guidelines%20and%20documentations.pdf?sequence=2>.
- [25] Danish Energy Agency. “Offshore Wind Potential in the North Sea”. In: (2024). URL: <https://ens.dk/media/2414/download>.
- [26] Danish Energy Agency. *Technology Data for Generation of Electricity and District Heating*. Apr. 2024. URL: <https://ens.dk/en/analyses-and-statistics/technology-data-generation-electricity-and-district-heating>.
- [27] Danish Energy Agency. *Technology Data for Energy Storage*. Sept. 2018. URL: <https://ens.dk/en/our-services/projections-and-models/technology-data/technology-data-energy-storage>.
- [28] Donald R. Woods. *Rules of thumb in engineering practice*. eng. Chichester: John Wiley [distributor], 2007. ISBN: 978-3-527-31220-7 978-3-527-61112-6 978-3-527-61111-9. DOI: 10.1002/9783527611119.
- [29] Danish Energy Agency. *Technology Data for Carbon Capture, Transport and Storage*. Nov. 2021. URL: <https://ens.dk/en/analyses-and-statistics/technology-data-carbon-capture-transport-and-storage>.

- [30] Danish Energy Agency. *Technology Data for Renewable Fuels*. Sept. 2018. URL: <https://ens.dk/en/analyses-and-statistics/technology-data-renewable-fuels>.
- [31] Eurostat. *Consumer Prices - Inflation*. URL: https://ec.europa.eu/eurostat/statistics-explained/index.php?title=Consumer_prices_-_inflation.
- [32] Danish Energy Agency. “The Danish Levelized Cost of Energy Calculator”. In: (2024). URL: <https://ens.dk/media/5653/download>.
- [33] S. Jalal Kazempour and Antonio J. Conejo. “Strategic Generation Investment Under Uncertainty Via Benders Decomposition”. In: *IEEE Transactions on Power Systems* 27.1 (Feb. 2012), pp. 424–432. ISSN: 0885-8950, 1558-0679. DOI: 10.1109/TPWRS.2011.2159251. URL: <http://ieeexplore.ieee.org/document/5937035/> (visited on 02/22/2025).
- [34] Seungwoo Kang et al. *Innovation outlook: renewable methanol*. eng. Ed. by Dolf Gielen and Greg Dolan. Abu Dhabi: International Renewable Energy Agency, 2021. ISBN: 978-92-9260-320-5.
- [35] Fangfang Li et al. “Energy, Cost, and Environmental Assessments of Methanol Production via Electrochemical Reduction of CO₂ from Biosyngas”. en. In: *ACS Sustainable Chemistry & Engineering* 11.7 (Feb. 2023), pp. 2810–2818. ISSN: 2168-0485, 2168-0485. DOI: 10.1021/acssuschemeng.2c05968. URL: <https://pubs.acs.org/doi/10.1021/acssuschemeng.2c05968> (visited on 02/21/2025).